

### **RESEARCH ARTICLE**

## SPECIAL ISSUE: CELL BIOLOGY OF HOST-PATHOGEN INTERACTIONS

# Human microsporidian pathogen *Encephalitozoon intestinalis* impinges on enterocyte membrane trafficking and signaling

Juan Flores<sup>1,\*</sup>, Peter M. Takvorian<sup>1,2,\*</sup>, Louis M. Weiss<sup>2</sup>, Ann Cali<sup>1,‡</sup> and Nan Gao<sup>1,‡</sup>

#### **ABSTRACT**

Microsporidia are a large phylum of obligate intracellular parasites. Approximately a dozen species of microsporidia infect humans, where they are responsible for a variety of diseases and occasionally death, especially in immunocompromised individuals. To better understand the impact of microsporidia on human cells, we infected human colonic Caco2 cells with *Encephalitozoon intestinalis*, and showed that these enterocyte cultures can be used to recapitulate the life cycle of the parasite, including the spread of infection with infective spores. Using transmission electron microscopy, we describe this lifecycle and demonstrate nuclear, mitochondrial and microvillar alterations by this pathogen. We also analyzed the transcriptome of infected cells to reveal host cell signaling alterations upon infection. These high-resolution imaging and transcriptional profiling analysis shed light on the impact of the microsporidial infection on its primary human target cell type.

This article has an associated First Person interview with the first authors of the paper.

KEY WORDS: Microsporidia, *Encephalitozoon intestinalis*, Autoinfective spores, Host–pathogen interactions, Mitochondria, Enterocyte, Brush border, Membrane trafficking, Transcriptomics

### INTRODUCTION

Microsporidia are a phylum of eukaryotic obligate intracellular pathogens of animals and man. They form environmentally resistant spores transmissible to new hosts through food or water (Cali and Takvorian, 2004, 2014; Fayer and Santin-Duran, 2014). Phylogenetic analysis suggests that microsporidia are closely related to Fungi and are closely related to the Cryptomycota (Keeling et al., 2014; Han and Weiss, 2017). Over 200 genera and 1400 species of microsporidia have been described, and they are found in every major animal group including humans (Becnel et al., 2014).

In humans, microsporidiosis occurs worldwide. The prevalence and geographic distribution of infection are variable due to diagnostic methods and population demographics (Bednarska et al., 2014; Didier and Weiss, 2006; Fayer and Santin-Duran, 2014). Nine genera, containing 17 species, have been identified to cause microsporidiosis in humans (Fayer and Santin-Duran, 2014; Han et al., 2020). Gastrointestinal infection is the most common presenting symptom and this is usually due to either *Enterocytozoon* 

D N.G., 0000-0003-4264-7438

Handling Editor: Derek Walsh Received 1 September 2020; Accepted 1 February 2021 bieneusi or Encephalitozoon intestinalis. Enterocytozoon bieneusi is the cause of most human infections and it infects the biliary tract and small intestine, causing chronic diarrhea (Desportes et al., 1985; Orenstein et al., 1990). Unfortunately, it has not been successfully propagated in cell culture or laboratory animals including immunesuppressed mice (Visvesvara, 2002), greatly limiting its study.

Encephalitozoon intestinalis, formerly known as Septata intestinalis (Cali et al., 1993; Hartskeerl et al., 1995) can cause intestinal infection with associated dissemination to other organs. Encephalitozoon intestinalis infects both immune competent and immunecompromised individuals. Interestingly, E. intestinalis infection was found in 30% of patients with Crohn's disease (Andreu-Ballester et al., 2013). Encephalitozoon intestinalis infects enterocytes, its primary target cell type, causing diarrhea. In immune-compromised individuals, especially in those with advanced AIDS, E. intestinalis infection can lead to severe enteritis, disseminating infections in kidney and in hepatobiliary tract (Cali et al., 1993; El Fakhry et al., 2001; Hamamci et al., 2015; Raynaud et al., 1998; van Gool et al., 1997). It can also be responsible for eye and liver infections (Didier and Weiss, 2006). While Enterocytozoon bieneusi has not been propagated continuously in culture, E. intestinalis, like other Encephalitozoon species, grows in some mammalian cell lines, such as RK13, but continuous culture in human enterocyte has not been established.

Enterocytes are the mature intestinal epithelial cells that line the small intestinal and colonic mucosa. They are critically important for nutrient absorption and their barrier function. As intestinal epithelium is constantly exposed to chemicals, pathogens and assorted damaging materials, mature epithelial cells are sloughed off and undergo constant renewal from stem cells that undergo a cycle of differentiation. One identifying feature of differentiated enterocytes is the presence of apical arrays of microvilli that form brush borders. The nuclei of these polarized enterocytes are located in the basal portion of the cells (Crawley et al., 2014). Caco2 cells are a human enterocyte-like colonic epithelial cell line that undergoes differentiation and polarization (Gao and Kaestner, 2010; Knowles et al., 2015). Two initial studies of E. intestinalis utilizing Caco2 cells described the spore-host cell surface interaction and factors related to spore germination (Foucault and Drancourt, 2000; Leitch et al., 2005). Unfortunately, neither study provided ultrastructural images of the parasite or documented its life cycle within Caco2 cells or interaction with the host organelles.

There has been a general lack of understanding of human-microsporidial molecular interactions. The majority of observations on microsporidial—host molecular relationships have been demonstrated in the nematode, *Caenorhabditis elegans* (Botts et al., 2016; Kuo et al., 2018; Reddy et al., 2019), insects and zebrafish (Troemel, 2011). Watson et al. (2015), reported on the evolution of microsporidial gene expression of *Trachipleistophora hominis* grown in rabbit kidney cells (RK-13). They reported that *T. hominis* has ~30% more genes than the 'small genome' microsporidia, such as *Encephalitozoon*. They also observed an overall reduction of gene activity of infected cells, except for genes

<sup>&</sup>lt;sup>1</sup>Department of Biological Sciences, Rutgers University, Newark, New Jersey 07102, USA. <sup>2</sup>Departments of Medicine and Pathology, Albert Einstein College of Medicine Bronx, New York 10461, USA.

<sup>\*</sup>These authors contributed equally to this work

<sup>&</sup>lt;sup>‡</sup>Authors for correspondence (anncali@newark.rutgers.edu; ngao@rutgers.edu)

that increase ATP production and other metabolites utilized by the parasite (Watson et al., 2015).

Despite the overt human pathologies associated with microsporidia in general and, more specifically, E. intestinalis infection, it remains unknown how these pathogens impact enterocytes at the molecular and ultrastructural level. Studies of the complete developmental cycle of E. intestinalis, its utilization of host organelles and subsequent parasite-induced pathologies in a human enterocyte model should enhance our understanding of how microsporidia, such as E. intestinalis, alter enterocyte function and hijack host organelles for propagation and dissemination. Herein, we report the development of a system for the continuous culture of E. intestinalis in Caco2 cells. In this system, we demonstrate that E. intestinalis infection of Caco2 cells recapitulated the in vivo life cycle of E. intestinalis. Additionally, we identified two types of spore development – typical environmental spores that leave the host, and autoinfective spores that immediately germinate, spreading infection to neighboring cells. Furthermore, we found that infection altered the host cell mitochondria, nucleus and brush-boarder structures. Genome-wide untargeted transcriptomic analysis demonstrated that E. intestinalis infection had an impact on cell signaling networks related to energy, metabolism and membrane trafficking.

#### **RESULTS**

# E. intestinalis infects Caco2 cells recapitulating the in vivo life cycle

To gain mechanistic insights into *E. intestinalis* development and induced pathology in its natural human host cell targets, Caco2 cells were grown to confluence in culture flasks or on cover glasses, prior to infection with *E. intestinalis*. Visualization through fluorescence staining for the actin cytoskeleton, as an indicator for the monolayer, was performed by incubation of fixed uninfected Caco2 and *E. intestinalis*-infected cells with -halloidin–Alexa Fluor 488. Spores were identified by staining with Calcofluor White 2MR, which stains the chitin that is present in the spore wall. Uninfected Caco2 cells displayed a typical confluent monolayer arrangement and chitin was not present (Fig. 1A).

Transmission electron microscopy (TEM) examination of uninfected cells revealed enterocytes in various stages of differentiation. Immature cells were small, rounded and contained a large oval nucleus surrounded by a thin layer of cytoplasm (Fig. 1B). Cells undergoing differentiation displayed a morphological initiation of polarization. They were elongated, with the nucleus positioned towards the basal part of the cells, while showing some microvilli on the apical surface (Fig. 1C). Fully differentiated cells were elongated with organized microvilli that formed a well-defined apical brush border (Fig. 1D).

At 2 weeks after *E. intestinalis* inoculation, infected Caco2 monolayers were vacuolated and numerous cells were found to contain clusters of spores in vacuoles identified by Calcofluor White 2MR staining (red, Fig. 1E). Close examination detected intracellular scattered spores (white arrowhead, Fig. 1G) as well as spores in the extracellular space close to the plasmalemma (open arrowheads, Fig. 1F,G).

The *in vivo* infection cycle of *E. intestinalis* in human enterocytes (Fig. 1H) starts with spores infecting cells and forming a parasitophorous vacuole (PV) inside the host cell cytoplasm, where the parasite proliferates, then undergoes sporogonic development, ending in production of new infective spores (Cali and Takvorian, 2014).

TEM examination of infected cells revealed one or multiple parasites in the PV within the host cell cytoplasm. We noted that infected cells demonstrated a curved or crescent-shaped host nuclei

with a sporoplasm or early PV tightly nested against the invaginated portion of the nucleus (Fig. 1I,J). The *E. intestinalis* PV contained parasites at different developmental stages with proliferative, sporogonic and mature spores present (Fig. 1K). Some spores, while inside the PV, extruded their polar tubes, which often exited the PV and on occasion, the infected host cell. This indicates that two spore populations develop within the cell, one reflecting an autoinfective feature and the other for environmental dissemination outside the host (Fig. 1L). *Encephalitozoon intestinalis* infection *in vitro* in these enterocyte-like human Caco2 cells contained mature PVs with all the developmental and sporogonic stages of *E. intestinalis*, recapturing the *in vivo* life cycle as illustrated in Fig. 1H.

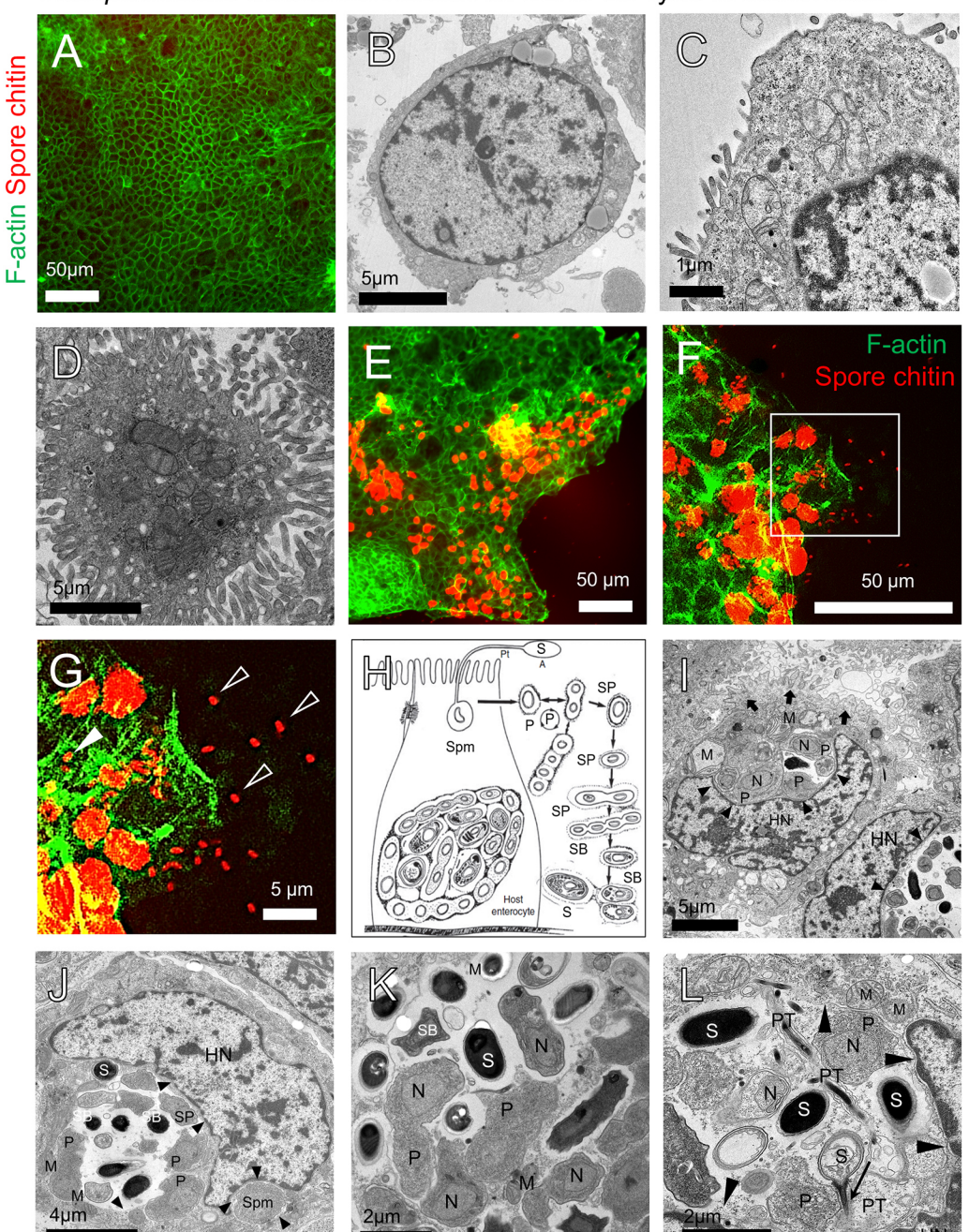
## Global alteration of host cell transcriptome by Encephalitozoon intestinalis

To understand the impact of *E. intestinalis* infection on host cells at the molecular level, we performed bulk RNA sequencing (RNAseq) analysis on uninfected (n=4) and infected Caco2 cell cultures (n=3), harvested in two independent experiments. Principal component analysis (PCA) revealed distinct clustering of the E. intestinalisinfected samples (red) from uninfected cells (blue) (Fig. 2A) and a volcano plot demonstrated the distribution of 17,836 genes by fold changes and P-values (Fig. 2B). Genes showing the most dramatic increase were involved in proliferation, such as CD44 (Lv et al., 2016), NPTX1 (Peng et al., 2018) and MYEOV (Moss et al., 2006). In contrast, genes showing the most significant reduction were involved in anti-proliferation, including KNG1 (Xu et al., 2018), CUBN (Gremel et al., 2017) and CYP2C9, suggesting that E. intestinalis infection stimulated host cell proliferation. Differential gene expression and heatmap analysis demonstrated that 269 genes increased by at least 1.5-fold and that 461 genes decreased by at least 1.5-fold, compared to levels in uninfected cells (P<0.05) (Fig. 2C).

Untargeted gene set enrichment analysis (GSEA) revealed that E. intestinalis infection significantly activated host gene networks denoted as (i) synaptic and presynaptic membrane formation; (ii) clathrin adaptor complex and vesicle coat; (iii) the phagocytic cup and extracellular organelles; (iv) mitochondrial respiratory chain; (v) SNARE complex; (vi) cell cortex, midbody and centriolar structural components; and (vii) AMPA glutamate receptor complex (Fig. 2D). This suggests that *E. intestinalis* strongly promoted the formation of host-pathogen interfacing membranes and host mitochondrial respiration. Encephalitozoon intestinalis infection suppressed gene networks that were responsible for (i) the nuclear membrane components; (ii) the formation of mature cellular membrane structures, including brush border, lamellar body and apical membrane; (iii) endo-lysosomal functions, including various proton pumps, membrane and lumen components, and (iv) the mechanistic target of rapamycin (mTOR) complex (Fig. 2E). These genome-wide transcriptomic analyses suggested that E. intestinalis rewired host cell mitochondrial energy production and membrane trafficking in favor of parasitic development. Interestingly, the gene angiotensin converting enzyme 2 (ACE2) is downregulated in Caco2 cells infected with E. intestinalis. The protein encoded by this gene has more recently received attention because of its role as the receptor binding partner for the S-protein on the SARS-CoV2 virus responsible for the 2020 pandemic (Bourgonje et al., 2020).

# E. intestinalis recruits host mitochondria and alters respiration

Our RNA-seq data suggested that *E. intestinalis* infection has a significant effect on host mitochondrial function. Consequently, we sought to determine by TEM whether there was an observable



# Encephalitozoon intestinalis establishes active life-cycle in Caco2 cells.

Fig. 1. See next page for legend.

morphological feature that could be correlated with this observation during infection. We found that the mitochondria of cells containing parasites at the early developmental stage appeared to be recruited by the parasites and accumulated around the sporoplasm (Fig. 3A) and mitochondria tightly abutted the newly formed PV membrane adjacent to proliferative parasites, which were attached to the inner portion of the PV membrane (Fig. 3B). During the stages of parasite proliferative, some mitochondria had alternating electron dense and lucent structure that appeared to connect to the proliferative parasite membrane (Fig. 3C), while others developed thin tubular structures interfacing with the PV membrane (Fig. 3D). Prolonged infection and interaction with parasites induced a number of pronounced

morphological changes in mitochondria, such as aberrant geometrically shaped cristae membranes, loss of cristae and severe swelling (Fig. 3B–D). Approximately 70% of mitochondria in infected cells exhibited these abnormalities (Fig. 3E), suggesting that host mitochondrial machinery was being modified by infection.

To determine what molecular modifications were exerted by *E. intestinalis* on host mitochondria, we interrogated mitochondriarelated gene sets that underwent significant changes in infected cells. First, there was a systemic elevation of genes contributing to the intrinsic components of mitochondrial membrane (Fig. 3F,I). The elevated *IMMT* (An et al., 2012), *CHCHD3* (Darshi et al., 2011),

Fig. 1. E. intestinalis establishes an active life-cycle in Caco2 cells. Uninfected (control) and Encephalitozoon intestinalis-infected Caco2 cells were grown to confluence and fixed 21 days after seeding the cultures on coverslip chamber slides. Both cultures were immunostained with phalloidin-Alexa Fluor 488 for actin and Calcofluor White 2MR for chitin and examined by fluorescencemicroscopy. Additionally, control and infected cells were also grown in cell culture flasks for TEM processing and examination. (A) Fluorescence image of uninfected phalloidin and Calcofluor White-stained cells showing a typical confluent monolayer arrangement with chitin not present, indicating an absence of infection in the Caco2 cells. (B-D) TEM examination of uninfected cells revealed Caco2 cells in different stages of differentiation. (B) Immature cells were small, rounded, and contained a large oval nucleus surrounded by a thin layer of cytoplasm. The cell surface lacked microvilli and exhibits no signs of polarity. (C) Caco2 cell in an early stage of differentiation. The cell is slightly elongated, the nucleus is more distally located, and a few microvilli are present on the apical surface. (D) A sagital section through a well-differentiated cell covered with tightly packed microvilli. (E) At 2 weeks after E. intestinalis inoculation, phalloidin-stained infected Caco2 monolayers were vacuolated and exhibited scattered infections identified by immunostaining of Calcofluor White 2MR for the spore wall chitin (red). Clusters of spores inside parasitophorous vacuoles (PV) and individual spores outside the cells (enlargement) were visible, indicating E. intestinalis undergoes a complete development in caco-2 cells. (F,G) A region at the periphery of the monolayer where individual spores can be seen both intracellularly (white arrowhead in G) and extracellularly (open arrowheads in G). (H) A diagrammatic representation of the in vivo E. intestinalis life cycle in human enterocytes is included to illustrate the stages of parasite development and their association with a PV that isolates the developing organisms from direct contact with the host cell cytoplasm. The cycle commences when a spore (S) germinates and a sporoplasm is injected into the host cell via the polar tube (Pt). The parasite sporoplasm (Spm) produces a PV that is not obvious until cell multiplication occurs. As the parasite's proliferative development (P) continues, the organisms appear tightly abutted to the PV limiting membrane until the beginning of sporogony, which is morphologically identified by electron dense secretions on the developing sporont (SP) cell surface and the detachment of the parasite cell from the PV. In sporogony the parasite cells may divide one or two times producing two to four sporoblast cells (SB) which metamorphose into spores (S). In this life cycle, both environmental (spores that leave the host) and autoinfective spores occur. That is, some spores immediately germinate, extruding their polar tubes and thus inoculate other host cells, repeating the infective process. Diagram is adapted from Cali and Takvorian, 2014 with permission from John Wiley and Sons. (I) TEM examination of infected Caco2 cells revealed a horseshoe shaped host nuclei (HN) and well-developed PVs containing numerous organisms. The upper cell PV contains several proliferating (P) stages of uninucleate (N) parasites. The arrowheads indicate the location of the PV membrane-host interface. The broad arrows indicate the abnormal (shortened, wide and disorganized) microvilli. The host nuclei of both cells have formed a crescent shape that encompasses a significant portion of the PV. Several mitochondria (M) abut the PV membrane. The PV in the lower cell contains organisms that are in various stages of sporogany, sporoblasts (SB) and spores (S). (J) Caco2 cell with a large well-formed PV containing all stages of E. intestinalis development partially encircled by a horseshoe shaped HN. The section of the PV that contains proliferative organisms has mitochondria (M) abutted to it. Note a sporoplasm (Spm) is tightly abutted to the lower portion of the HN and is forming an invagination where the parasite PV will interface with the HN. Arrowheads indicate where the PV interfaces with HN. (K) PV containing E. intestinalis at several stages of development. The PV also contains amorphous material between some organisms, typical of E. intestinalis. Note several of the elongated proliferative (P) cells are in the process of cytokinesis. (L) Infected Caco2 with a PV containing extruded PTs. The PV membrane (long arrowheads) abuts the curved HN and host cytoplasm containing numerous mitochondria (M). Inside the PV are organisms in the proliferative (P) and sporogonic stages of development. Several spores (S) are also present, indicating the parasite has undergone a complete developmental cycle. Several extruded polar tubules (PT) enclosed by membranes are present in the PV. The presence of extruded PTs indicate that some spores are auto-infective, they discharge their contents while inside the host cell to initiate secondary infections or exit the PV and infect neighboring cells. In the lower portion of the PV is an empty auto-infective spore (S) with a portion of its discharged PT (arrow) still attached to the spore shell.

CHCHD6 (An et al., 2012) and CHCHD10 (Genin et al., 2016) genes all encode scaffolding proteins with known involvement in the maintenance of mitochondrial cristae morphology (Fig. 3I). There was increased PISD, which encodes a protein that normally catalyzes the conversion of phosphatidylserine to phosphatidylethanolamine on the inner mitochondrial membrane, while AGK, which was also increased, works with the TIMM22 complex to assemble proteins in the mitochondrial membrane.

In addition to mitochondrial membrane components, the genes encoding TIMM17A, TIMM17B (Bomer et al., 1996; Moro et al., 1999), TIMM23 (Bauer et al., 1999; Yamamoto et al., 2002) and SLC25A4 (Willis et al., 2018), which are involved in the maintenance and assembly of protein complexes necessary for ATP production, were also increased in infected cells (Fig. 3I). As microsporidia are known to use host ATP, consistent with an overt attempt to elevate mitochondrial ATP production, genes contributing to the mitochondrial respiratory chain complex I (also known as type I NADH dehydrogenase), were increased upon infection with the parasites (Fig. 3G,H,J). The complex is responsible for the transfer of electrons from NADH to coenzyme Q10 and the transport of protons across inner mitochondrial membrane. The elevated complex I gene network is exemplified by the increase seen in the NDUFC genes, which are responsible for the formation of the core catalytic subunit of complex I (Fig. 3H,J), NDUFV1, which encodes another complex I-forming oxidoreductase on the matrix side of the mitochondria, and mitochondrial nuclear-destabilizing factors (MT-NDFs), which are believed to be critical for ATP production (Sazanov, 2015). The chaperone-encoding gene PARK7, which helps stabilize complex I (Junn et al., 2009), was also increased in infected cells.

Elevations of the above mitochondrial membrane and respiratory chain components reflect a de novo biogenesis of mitochondria in infected cells, possibly an attempt to replace parasite-damaged mitochondrial organelles or the parasite increasing host energy supply. Two genes encoding master regulators of mitophagy, AFG3L2 and PINK1, were both activated in infected cells (Fig. 31). During mitophagy, damaged mitochondria are selectively degraded by autophagosomes. The cleavage of PINK1 by AFG3L2 initiates a signaling cascade driving mitophagy. In line with this, FIS1, another critical regulator of membrane fusion with lysosome during mitophagy (Xian et al., 2019), was also increased in infected cells (Fig. 3I). Staining for mitochondrial reactive oxygen species (ROS) by using CM-H<sub>2</sub>Xros (a Mitotracker) suggested a two-fold elevation of mitochondrial counts in infected cells (Fig. 3K). Thus, there was a strong tendency for E. intestinalis to recruit, hijack and stimulate the reproduction of host mitochondria.

The parasites appeared to also affect mitochondrial function via increasing membrane permeability and transport across mitochondria. This was exemplified by elevated levels of genes encoding SPG7 (Fig. 3I), a metalloprotease regulating mitochondrial permeability (Hurst et al., 2019), ABCB6, which binds to heme and porphyrins to facilitate ATP uptake into mitochondria (Krishnamurthy et al., 2006), and MPC1, which regulates pyruvate transport into the mitochondria (Koh et al., 2018) (Fig. 3I). In addition, BAK1 that promotes mitochondrial outer membrane permeabilization was also increased.

Furthermore, TEM-revealed recruitment of mitochondria by *E. intestinalis* was also reflected at the molecular level. *Encephalitozoon intestinalis* appeared to activate genes encoding RHOT1, which aids the anterograde transport of mitochondria (Grossmann et al., 2020), and MGARP, which facilitates kinesindependent mitochondrial trafficking along microtubules in infected cells (Li et al., 2009) (Fig. 3I). These data support that *E. intestinalis* robustly alters host mitochondrial biogenesis and ATP production.

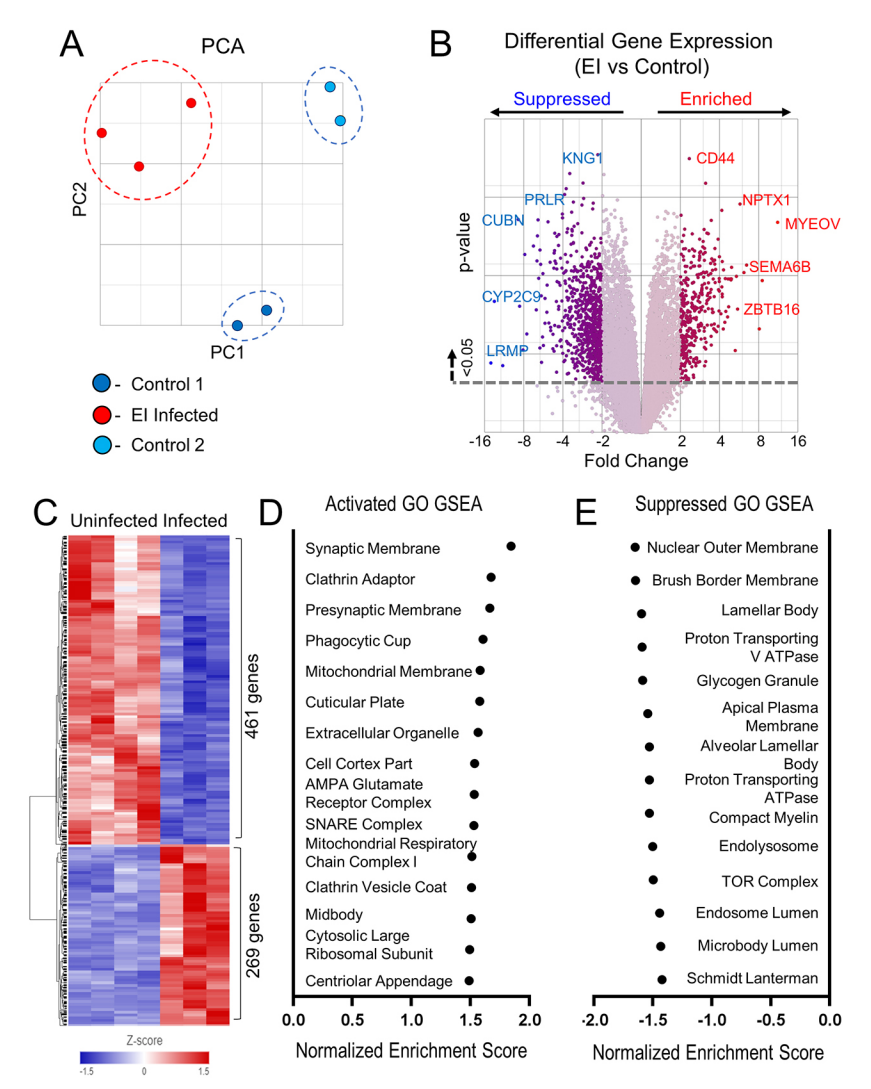


Fig. 2. Global alteration of transcriptome by E. intestinalis. Sequencing was undertaken on uninfected (n=4) and infected (EI) (n=3) Caco2 cells. (A) Principal Component Analysis (PCA) of four uninfected samples (blue and light blue) and infected (red). (B) Volcano plot of differential gene expression in infected compared to uninfected. Highlighted points are genes with fold change <-1.5 or >1.5; P<0.05 (C) Heatmap based on RNA-seq data of uninfected and infected Caco2 revealed 269 genes significantly downregulated and 461 genes significantly upregulated in the infected samples. (D) Gene ontology (GO) analysis identified significantly upregulated terms in infected samples including intrinsic component of the mitochondria, mitochondrial respiratory chain complex I, and the SNARE complex. (E) GO analysis identified significantly downregulated terms in infected samples including the nuclear outer membrane, brush border membrane, apical plasma membrane, and endolysosome. For GO analysis, terms were reported by GSEA as statistically significant at P<0.001

#### Unusual modification of host nucleus by E. intestinalis

One distinct TEM feature of E. intestinalis-infected cells was the presence of crescent- or horseshoe-shaped host nuclei abutted against an established PV containing developing organisms. Early infections, as indicated by the presence of a sporoplasm or early proliferative stages, abutted or adjacent to the host nucleus, had limited indentation (Fig. 4A). The parasite membrane did not appear to touch the host nuclear envelop (Fig. 4A). As the infecting stage advanced to the formation of a PV membrane, the host perinuclear membrane began to form an obvious indentation, and the PV membrane appeared to closely interface to the host nucleus (Fig. 4B). As the organisms (meronts) proliferate, they remain attached to the PV membrane, portions of which were then abutted to the host nucleus with nuclear pores often visible in this area (Fig. 4C). An indicator of microsporidial karyokinesis, is the presence of an electron-dense area of the parasite nuclear membrane, identified as a nuclear plaque (NP), which acts as a microtubule organizer, similar to a centriole (Fig. 4D). The presence of both meronts attached to the PV membrane and sporogonic stages free in the PV, indicates asynchronous development. At the point when organisms formed PV membrane, we found some PVs were almost completely engulfed by the host cell nuclei (Fig. 4D). A measurement of nuclear indentation at early and mature stages indicated a progression of this process (Fig. 4E).

These morphological events were also reflected at the molecular level. GSEA analysis illustrated a significant alteration of the nuclear outer membrane gene set in infected cells [P<0.05; normalized enrichment score (NES) of -1.37; Fig. 4F,H). Representative genes that were highly reduced by E. intestinalis included CDCC155 (Morimoto et al., 2012), and SYNE1, SYNE2, SYNE3 and SYNE4 (Horn et al., 2013; Morgan et al., 2011; Stewart-Hutchinson et al., 2008; Zhang et al., 2005), which interact with spectrins to act as mediators between the nuclear lamina and cytoskeleton (Fig. 4G,I). SNCA, a molecular chaperone specifically involved in the folding of synaptic fusion components of SNARE complex, and CLMN, a paralog of dystonin involved in spectrin and actin crosslinking and scaffolding were also reduced (Burré et al., 2010; Young et al., 2003). In addition, the E. intestinalis-induced nuclear indentation was consistent with altered SYNE genes, which belong to the linker of nucleoskeleton and cytoskeleton (LINC) complex, which controls the cytoskeletal rearrangement of perinuclear and nuclear space (Zhang et al., 2009). Three other genes in this functional set included LTC4S, for biosynthesis of leukotrienes (Welsch et al., 1994), RETSAT, for conversion of all-trans-retinol to all-trans-13,14,dehydroretinol (Moise et al., 2004), and *PSEN1*, which is responsible for cleavage of Notch receptors and APP (Fraering et al., 2004).

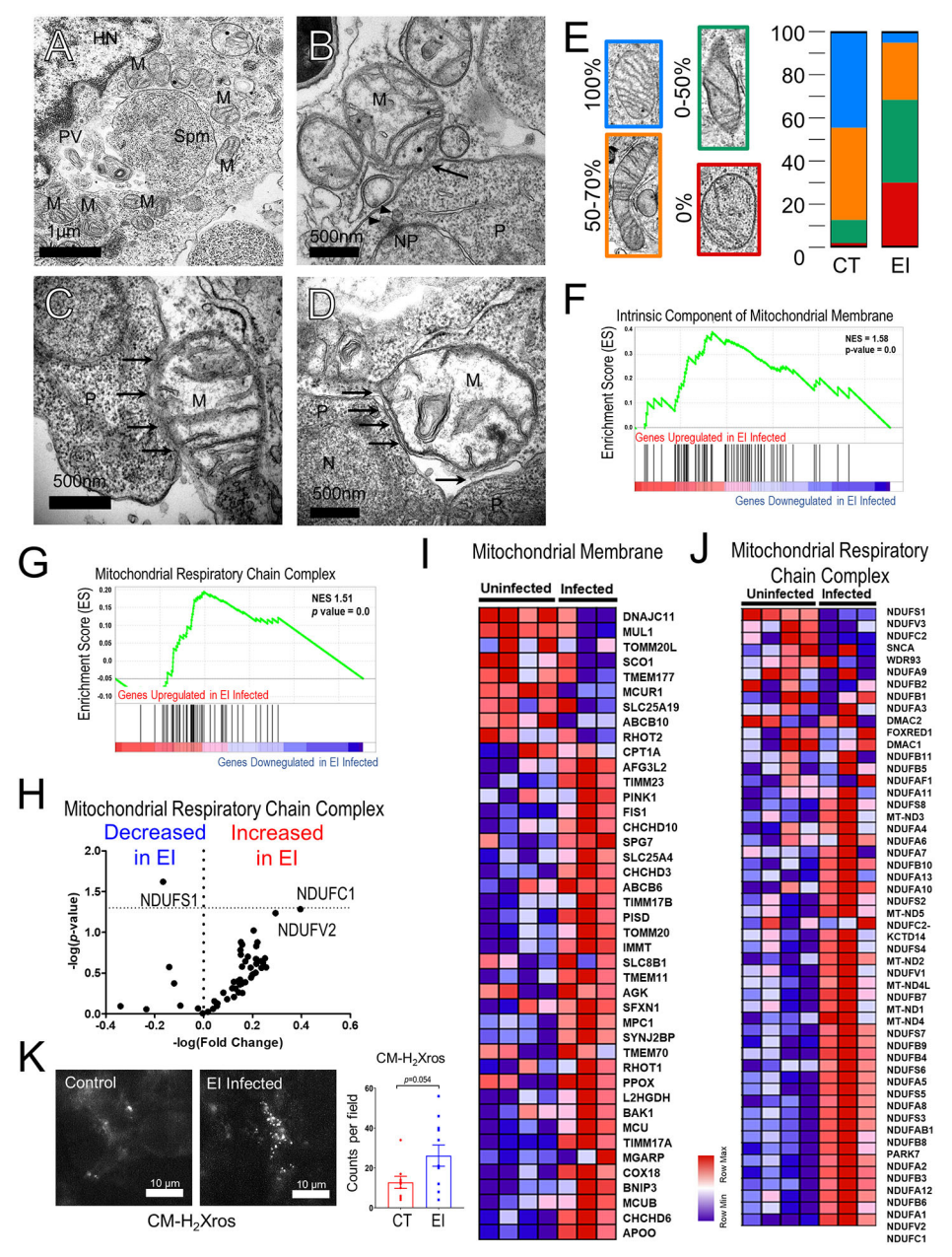


Fig. 3. Encephalitozoon intestinalis interacts and alters host mitochondria. *E. intestinalis* interface with Caco2 host cell mitochondria. (A) Sporoplasm (Spm) inside a PV adjacent to the host nucleus (HN). This thin section of the PV is surrounded by over 10 mitochondria (M) abutted to the PV membrane—cytoplasm interface. Several additional mitochondria are also in the surrounding cytoplasm. (B) Tight abutment of a mitochondrion (M) to a parasite limiting membrane (arrow). The parasite has a nuclear plaque (NP) with mitosomes (arrowheads) abutted to its nucleus (N); the presence of the NP indicates this is a proliferative cell that is in the process of or having just completed karyokinesis. Note the aberrant geometrical shaped cristae membranes in the mitochondria, indicating it is stressed. (C) Host mitochondrion (M) interfacing with an indentation (arrows) of the parasite membrane. (D) Host mitochondrion (M) interfacing with two proliferative (P) parasite cells. Fine tubular interconnections between the abutted membranes (arrows) are present. Note this mitochondrion also has aberrant geometrical shaped cristae membranes and appears to be under stress. (E) Quantification of mitochondrial cristae structure from EM imaging compared to control (CT). *E. intestinalis*-infected (EI) mitochondria were graded on cristae integrity based on four groups (outlined in examples, 100% being with intact cristae structure and 0% being completely absent). Note that CT cells have 90% normal mitochondria (blue and orange). Data represents EI (*n*=11) and CT (*n*=7) from two independent experiments. (F) GSEA shows enhanced expression of genes encoding for products found on mitochondrial outer membrane. (G) GSEA showed enhanced expression of gene products involved in formation of the mitochondrial respiratory chain complex I. (H) Volcano plot illustrating upregulated expression of genes described in G. (I,J) Heat maps illustrating upregulation of genes described in F and G. (K) Representative images of CM-H2Xros staining on conf

# E. intestinalis blocks apical transport, brush border morphogenesis and endolysosomal trafficking

TEM observations suggested that the normal apical brush borders developed in mature Caco2 cells (Fig. 5A,B), and that these were disrupted in *E. intestinalis*-infected cells (Fig. 5C,D). Consistent

with the TEM results, GSEA analysis revealed a global suppression of the cellular transcriptome for brush border morphogenesis (Fig. 5E,F). Reduction in the levels of *CDHR2* and *CDHR5*, which are responsible for the formation of inter-microvillus links (Crawley et al., 2014; Goldberg et al., 2000), was particularly consistent with

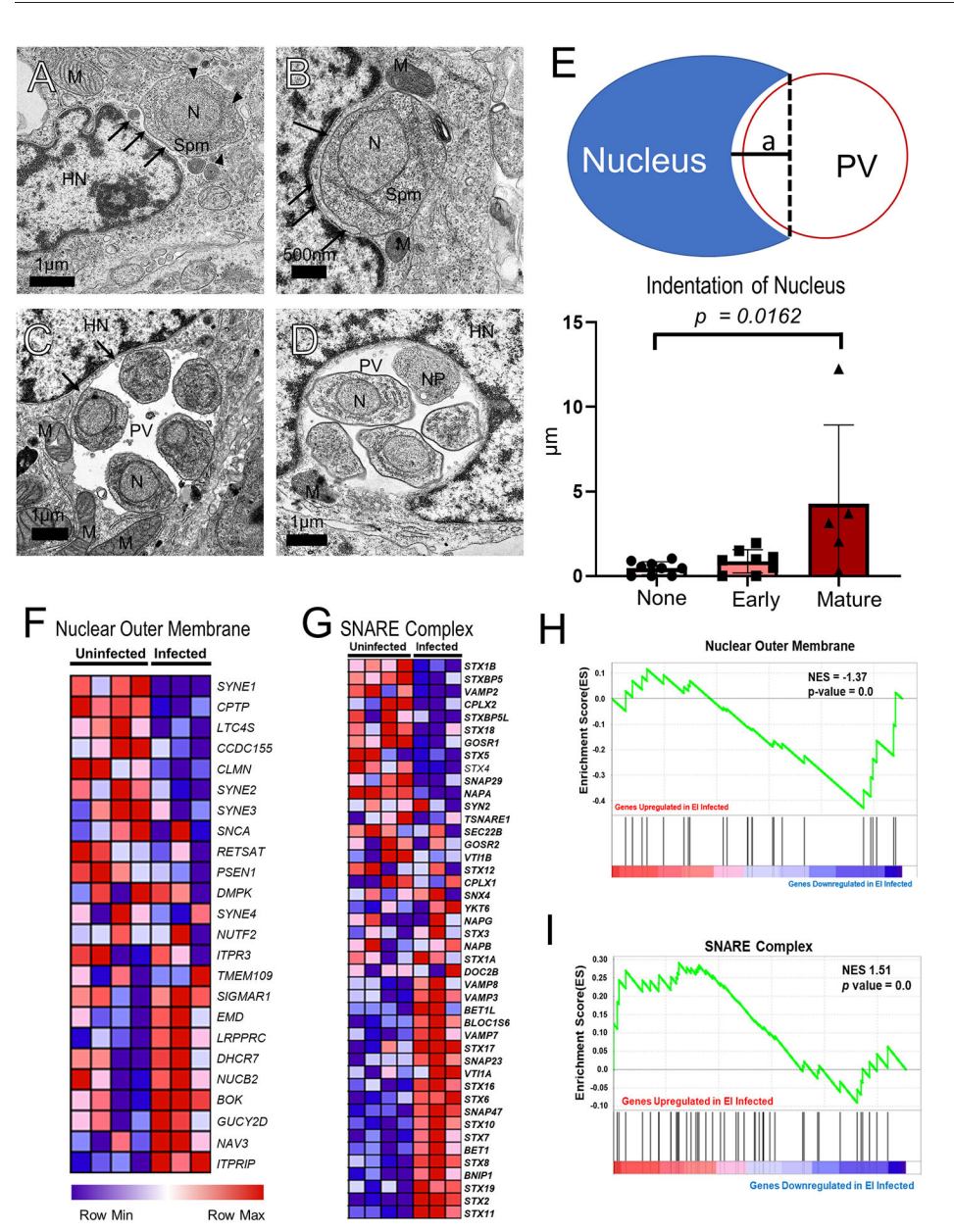


Fig. 4. E. intestinalis induces indentation of host cell nucleus. Early development of E. intestinalis in Caco2 cells and impact on host nucleus. (A) A sporoplasm (Spm) in close proximity to the host nucleus (HN). Note the HN is not indented. The arrows indicate a narrow space forming where the presumptive parasitophorous vacuole (PV) membrane will form. The arrowheads identify small segments of the PV membrane parasite-host cytoplasm interface. (B) A Spm abutted to a thin perinuclear membrane (arrows) outlining the indented portion of the HN. A mitochondrion (M) abuts the Spm membrane. (C) PV containing five proliferative parasite cells. These organisms are still attached to the PV membrane and several mitochondria are abutted to the PV membrane. Arrows indicate the thin PV membrane in close proximity to the host nucleus at a nuclear pore. (D) A portion of the host nucleus encircling a PV containing four organisms no longer attached to the PV membrane and that are covered with secretions. forming a slightly thicker limiting membrane. These features indicate they are becoming sporonts. The cell still attached to the PV membrane has a typical cell limiting membrane of a proliferative cell and a nuclear plaque (NP) from which microtubules form during karyokinesis, the presence of the NP indicates this is a cell that is in the process of karyokinesis or having just finished it. (E) Quantification of penetration of PV into the host nucleus in µm. Height (denoted as 'a') of the bottom of the concave portion of the nucleus was measured from the beginning of the host nuclear-PV interface. Bar graphs display mean±s.e.m. from two independent experiments, with individual measurement shown. P-value was calculated with a unpaired one-tailed t-test. (F,G) Heat maps of genes involved in formation of nuclear outer membrane and SNARE complex, respectively. (H,I) GSEA showed significantly enhanced expression of genes involved in nuclear outer membrane formation and membrane fusion, respectively.

the collapsed brush border structures in *E. intestinalis*-infected cells (Fig. 5C,D). A majority of the other genes with reduced levels encode proteins involved in transport of solutes (Hayashi and Yamashita, 2012; Schlingmann et al., 2002), hormones (Mahon et al., 2002) and nutrients (Drover et al., 2005; Lee et al., 1993; Qiu et al., 2006) across the apical membrane of mature enterocytes. Among them, *CUBN* encodes a brush-border localized receptor for vitamin B12. These data, under the context of a significantly reduced gene signature for apical plasma membrane (*P*<0.05; NES 1.53) suggested that *E. intestinalis* globally inhibited the apical membrane trafficking process in Caco2 cells (Fig. 5F,G).

In addition to apical transport, the reductions in the levels of gene encoding multiple adaptor proteins, including *AP2A2* and *AP2M1*, which regulate clathrin coat vesicles and vacuolar ATPase-dependent acidification of endolysosome (Aguet et al., 2013; Kadlecova et al., 2017), suggested a concomitant suppression of endocytic process by the parasites. Indeed, GSEA showed a significant reduction of the gene set related to the structure or function of endolysosome (Fig. 5H). Interestingly,

several endosome-dependent pathogen pattern recognition receptor genes, such *TLR3*, *TLR7* and *TLR9*, were also suppressed by *E. intestinalis*. Of note, and consistent with a suppressed endocytic pathway, our extensive TEM analysis failed to detect distinct lysosomes or autophagosomes in infected cells. Using a Lysotracker (Green DND-26), a pH-dependent fluorescent probe, we found reduced lysosomal staining events in infected cells (Fig. 51). These data collectively suggest that *E. intestinalis* not only hijacks and extracts mitochondrial energy through PV membrane fusion but appears to globally block host cell membrane trafficking and lysosomal function, presumably for its intracellular reproduction.

# E. intestinalis induces specific host defensive and reparative cascades

Because the top genes upregulated and downregulated by fold-change are involved in cell growth and suppression, respectively, we ran GSEA against the MSidDB hallmarks gene sets (Tables S1 and S2). Indeed, the Wnt/β-catenin along with Myc and late estrogen

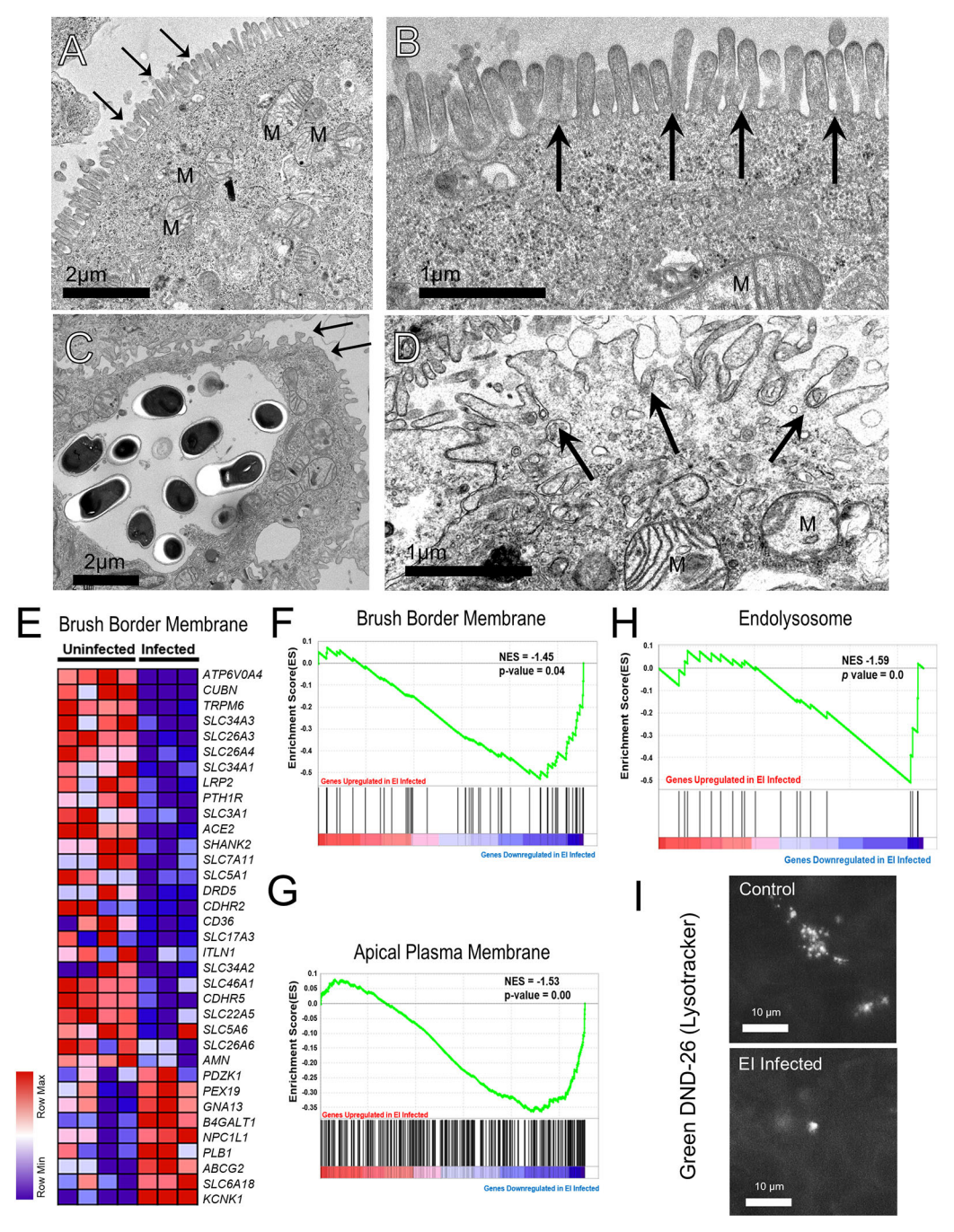


Fig. 5. *E. intestinalis* blocks apical and endolysosome trafficking. Comparison of Caco2 microvilli from control (uninfected) and infected cells. (A) Control Caco2 cell microvilli are well defined and evenly spaced (arrows). The underlying cytoplasm has a uniform granularity and mitochondria (M) with well-defined and organized cristae membranes. (B) Higher magnification image of the microvilli that form the brush border. (C) Infected Caco2 cell with aberrant 'club-like' microvilli (arrows) that are irregularly spaced. (D) Higher magnification of the aberrant microvilli (arrows) and underlying vaculated cytoplasm. Note the mitochondria are vacuolized and their cristae membranes are in geometrical arrangement, indicating these organelles are under stress. (E) GSEA heat maps illustrating suppression of genes related to products found in the portion of the plasma membrane surrounding the brush border in infected cells. (F) GSEA showing suppression of the same genes described in E. (G) GSEA showing suppression of gene related to products found in the apical plasma membrane of a cell. (H) GSEA showed suppression of gene products regulating endolysosomal formation. A Student's *t*-test was used to calculate *P*-values shown in F, G and H. (I) Representative images of Lysotracker DND-26 staining on confluent control (CT) and *E. intestinalis*-infected (EI) cultures.

response gene sets are significantly enriched in *E. intestinalis*-infected Caco2 cells (Fig. 6A–C). For example, the abundance of these following specific transcripts were increased in infected cells (please see Table S3 for a full list of differentially expressed genes). *GNAII* is a GTPase responsible for the inhibition of adenyl cyclase and plays a role in centrosome regulation during mitosis (Cho and

Kehrl, 2007). HEY1 is a transcription factor which was previously shown to be upregulated in colorectal cancer and associated with a poorer prognosis (Candy et al., 2013). Another transcription factor gene, histone deacetylase 11 (*HDAC1*) encodes a protein that is normally expressed in a tissue-specific manner and is found to be upregulated in several human cancer cell lines (Gao et al., 2002).

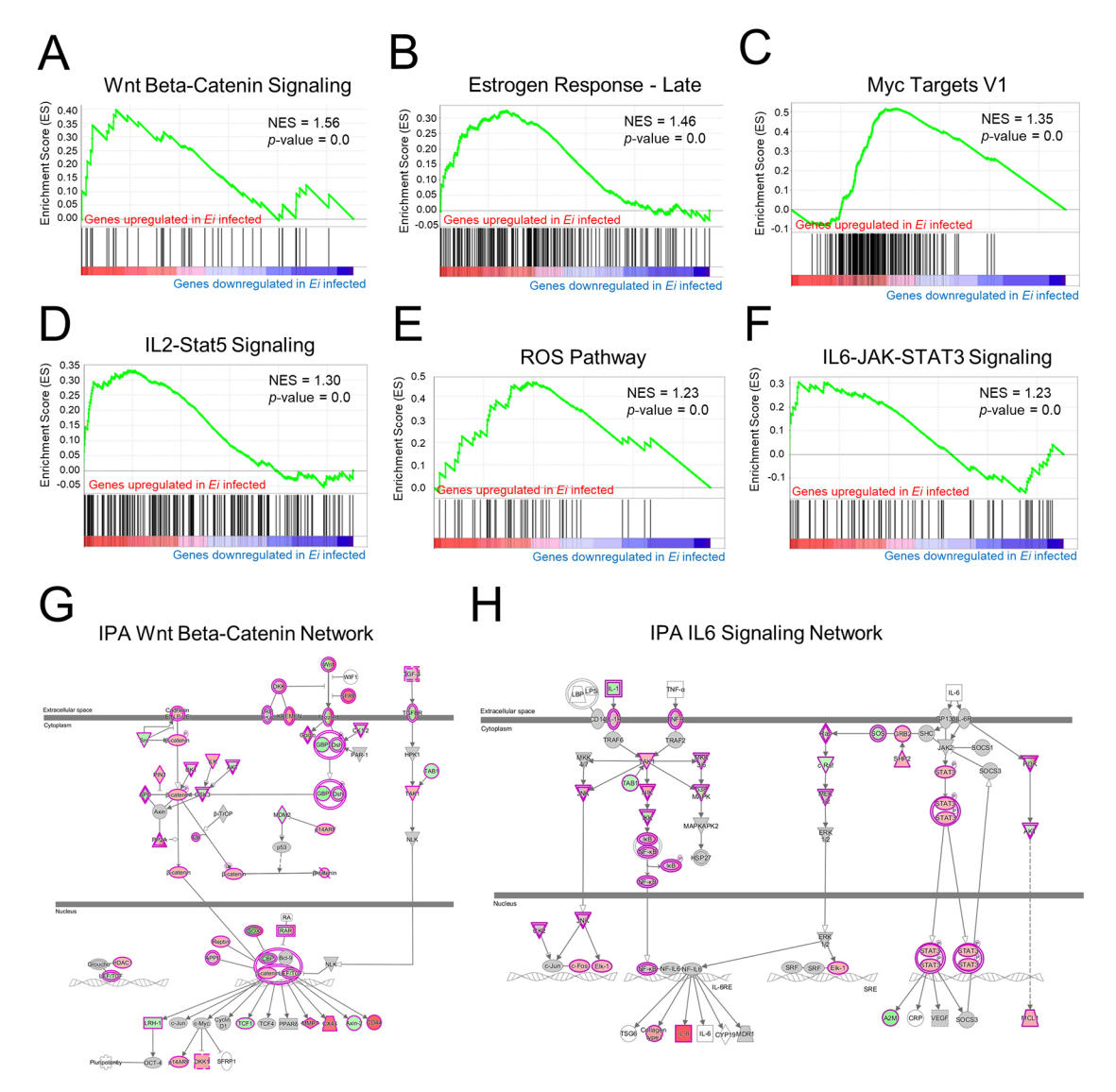


Fig. 6. *E. intestinalis* induces specific host defensive and reparative signal cascades. (A) GSEA showing upregulation of genes downstream of the WNT and β-catenin signaling pathway upon *E. intestinalis* (*Ei*) infection. (B) GSEA showing enhanced expression genes characteristic of a late response to estrogen upon *E. intestinalis* infection. (C) GSEA showing enhanced expression of a subgroup of genes regulated by Myc upon *E. intestinalis* infection. (D) GSEA showing enhanced expression of genes in the IL2–STAT5 signaling cascade upon *E. intestinalis* (*Ei*) infection. (E) GSEA showing enhanced expression of genes characteristically upregulated in response to ROS. (F) GSEA showing enhanced expression of genes of the IL6–STAT3 signaling pathway upon *E. intestinalis* infection. (G,H) Gene pathway analysis of Wnt/β-catenin signaling (G) and IL6 signaling (H). Red colored genes are overexpressed in *Ei*-infected Caco2 as compared to non-infected cells (control); green are suppressed.

Finally, *JAG1*, which encodes a well-characterized Notch1 and Notch2 receptor ligand and which was previously shown to be increased in APC<sup>min</sup> intestinal tumors (Guilmeau et al., 2010). Another Notch ligand, Delta-like1 (*DLL1*) is also upregulated (Table S3) and is known to be highly expressed in goblet cells in the intestinal epithelial tissue (Akiyama et al., 2010).

Similarly, cytokine pathways responding to pathogens (IL2-STAT5 and IL6–JAK–STAT3 and ROS gene sets) were significantly enriched in *E. intestinalis*-infected Caco2 (Fig. 6D–F). Genes upregulated in *E. intestinalis* infection include colony-stimulating factor 2 (*CSF2*), better known as *GM-CSF*, which is a well-known cytokine secreted in response to a variety of bacteria and viruses (Hsu et al., 1995). Additional genes that were increased in infected cells include the following, as shown in Table S3. Lymphotoxin β, CD79b and CD83 are known to promote lymphocyte survival and activation (Cragg et al., 2002; Pinho et al., 2014). *APLP1*, is a membrane associated

glycoprotein and has been previously shown to play a role in the dissemination of intestinal carcinoids (Arvidsson et al., 2008). *GLIPR2* enhances type 1 interferon signaling in response to TLR4 (Zhou et al., 2016). Genes found in the ROS hallmarks GSEA are primarily involved in reductase activity in response to an upregulation of ROS including *GLRX*, *GLRX2*, *TXNRD1* and *GPX4*. Additionally, the expression patterns of these genes have been shown to be dysregulated in studies focusing on colon cancer cell lines or tissue (Barrière et al., 2004; Cha and Kim, 2009; Peters et al., 2008).

Ingenuity pathway analysis (IPA) of our RNA-seq data was used to visualize members of the Wnt/β-catenin (Fig. 6G) and IL-6 (Fig. 6H) signaling pathways. A majority of the members in these pathways are significantly upregulated (red highlighted). Taken together, our GSEA and IPA analysis suggest that Caco2 cells respond to *E. intestinalis* infection by enhancing reparative and defensive signaling cascades.

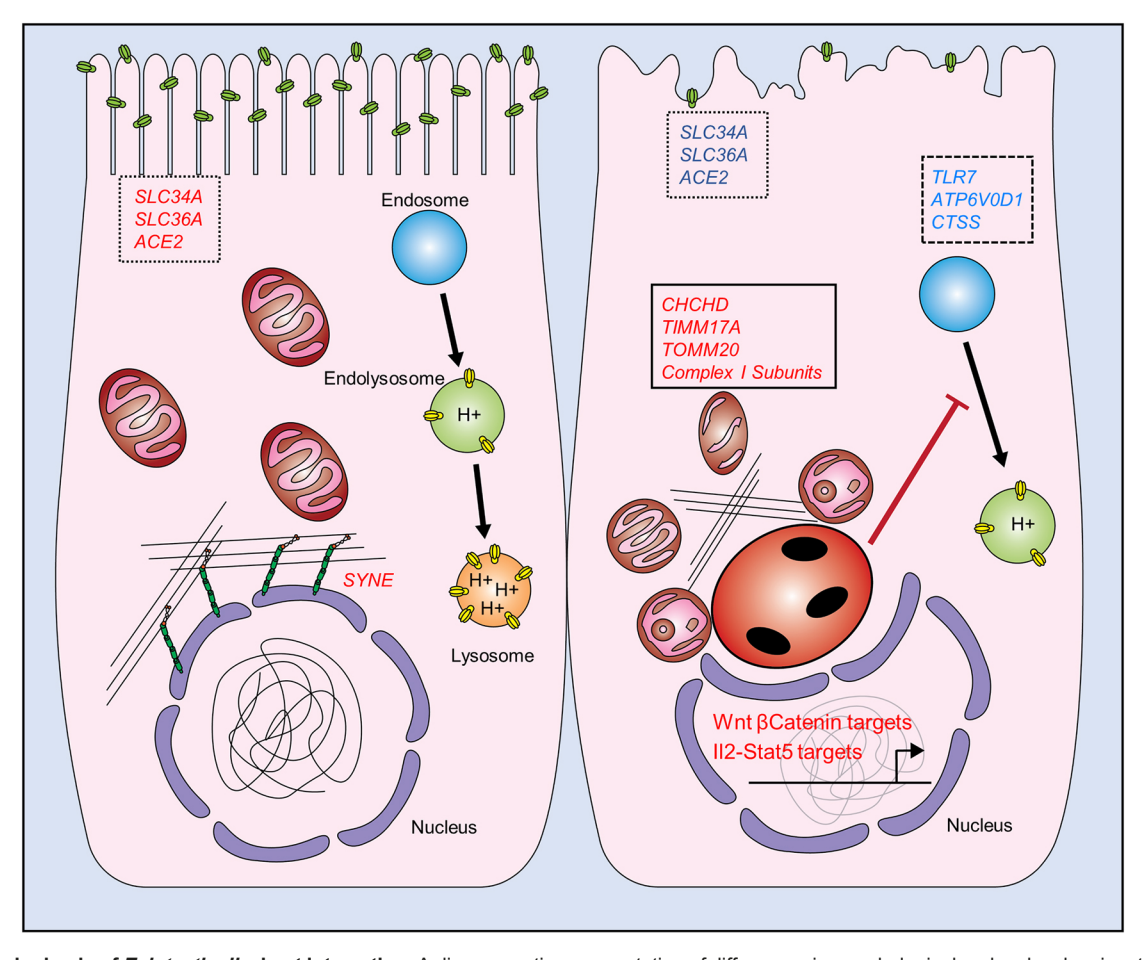


Fig. 7. Molecular basis of *E. intestinalis*—host interaction. A diagrammatic representation of differences in morphological and molecular signatures between Caco2 cells with (right) or without (left) *E. intestinalis* infection. Genes in red represent upregulated transcripts and blue downregulated. Uninfected enterocytes display uniform microvilli features including the expression of solute carriers typical of brush border membranes (dotted box). Upon infection, microvilli integrity is compromised, as well as endolysosomal formation and nuclear morphology. *E. intestinalis* infection results in reduced molecular signature of endolysosomes (dashed box), which may be linked to a decrease in V type ATPase transporters gene signatures. In contrast to mitochondria in uninfected enterocytes, *E. intestinalis*-infected Caco2 mitochondria display irregular morphology, including rounding and loss of cristae integrity. Infected Caco2 respond by upregulating genes (boxed) related to cristae structure maintenance. Finally, the host nucleus forms an invagination due to the presence of the growing PV (red oval structure). Nuclear outer membrane genes (*SYNE*) responsible for cytoskeletal-membrane interaction are lost in infected Caco2. Downstream targets of Wnt/β-catenin and IL2–STAT5 pathways are actively transcribed in response to the infection.

# DISCUSSION

E. intestinalis was first identified in human intestines of an HIV patient in 1993 (Cali et al., 1993). Early morphological study of E. intestinalis relied on the rabbit kidney RK13 cell line. Foucault and Drancourt (2000) reported that E. intestinalis uptake into Caco2 cells was by phagocytosis. Subsequently, Leitch et al. (2005) demonstrated that infection of these cells was by polar tube penetration with sporoplasm deposition, and suggested phagocytosis was not a significant factor for E. intestinalis infection. Both studies concentrated on initiation of infection. Consequently, neither of these reports described developmental stages, the life cycle, host cell–parasite interaction or pathology. Additionally, neither report provided ultrastructural images to support their position.

This current study utilized TEM to evaluate *E. intestinalis* infection in a Caco2 cell model and found that this method was able to capture most of its distinguishing *in vivo* life cycle features based on morphological analysis. Additionally, we demonstrate the presence of two types of spores – an environmental spore, which may exit the infected host in feces and eventually infect a new host, and auto-infective spores, which become activated and extrude their polar tube to spread infection inside the PV or upon release from a lysed cell.

Auto-infective spores may re-infect the host cell or neighboring cells, propagating infections in the host organism (Nigrelli, 1946). Unlike *E. bieneusi*, which primarily infects enterocytes, *E. intestinalis* often disseminates from enterocytes to other intestinal cell types, the liver, kidney, urinary tract, respiratory tract and eyes. These autoinfective spores may be responsible for the ability of *E. intestinalis* to disseminate. Furthermore, this represents one of the first studies systematically dissecting the molecular targets of *E. intestinalis* in a physiologically relevant human cell model. Our data suggest that *E. intestinalis* blocks the major membrane transport processed carried out by mature enterocytes, while preferentially establishing perinuclear vacuoles that directly engage the host nucleus and hijack host mitochondria. Several specific cellular signaling cascades were activated by *E. intestinalis*, potentially for defensive and reparative mechanisms (Fig. 7).

Microsporidia have undergone a minimization of their genome and cellular components, with one feature being their lack of traditional mitochondria, and they have been considered 'amitochondriate'. These organisms do, however, possess a mitochondrial remnant termed the 'mitosome', which retains the biosynthetic machinery for iron-sulfur clusters and some transport functions, but is no longer

involved in ATP production (Williams et al., 2014). A major open question regarding microsporidia—host interaction has been how these organisms interface and exploit host machinery for propagation. Microsporidial dependence on host organelles has been exemplified by the recruitment of host mitochondria (Hacker et al., 2014; Scanlon et al., 2004) and ER to the PV (Ferguson and Lucocq, 2019). This utilization and modification of host organelles has been reported in other intracellular pathogens, for example. Coxsackie viral infections (Hsu et al., 2010) and *Toxoplasma gondii* (Weiss and Kim, 2020). Likewise, we previously showed that during the development of the microsporidian *Anncaliia algerae* in human HeLa cells, they repurpose host microtubules and Golgi for parasite development (Santiana et al., 2016).

Microsporidial infection puts a tremendous stress on host mitochondria. The observed elevation of mitochondrial outer membrane and respiratory chain complex genes in the current studies suggests a cellular attempt to supply new mitochondria. Interfaces between host mitochondria and E. intestinalis are expected to allow ATP to flow to the parasite for its reproduction. Hacker et al. (2014) conducted an extensive study of mitochondrial binding with E. cuniculi PVs in rabbit cells (RK-13). They demonstrated that ATP and other metabolites were transported to proliferative stages by mitochondrial-PV voltage-dependent anion-channels. E. hellem sporoplasm surface protein 1 (EhSSP1) has been found to interact with mitochondrial voltage-dependent anion channels (VDACs) at the PV interface (Han et al., 2019). The current study showed an enrichment of ATP transporting proteins at the host cell–PV interface. Watson et al. (2015) reported a similar upregulation of host genes for proteins involved with glycolysis and ATP production in *T. hominis*-infected RK-13 cells.

While we and others have reported PV interaction with host mitochondria for E. cuniculi (Hacker et al., 2014), we describe here a similar phenomenon with respect to parasitic engagement with the host nuclear outer membrane (Fig. 7). Our data suggest that E. intestinalis potentially exploits the SNARE machinery to gain direct access and interface with host mitochondrial and nuclear membranes. Mechanistically, our TEM analysis revealed that the fusion between the PV membrane and host nuclear outer membrane was potentially facilitated by an activated SNARE network in infected cells. The expression of numerous syntaxins that are normally found in different intracellular membrane compartments were promoted by *E. intestinalis*. Among the elevated syntaxins, syntaxin 2 is known to localize in the perinuclear region (Band and Kuismanen, 2005), syntaxin 11 is present in late endosomes and trans-Golgi network (Valdez et al., 1999), and syntaxin 8 recycles claudin-16 at tight junctions in epithelial cells (Ikari et al., 2014). Furthermore, BNIP, an ER protein responsible to promote apoptosis when defective vesicle fusion occurs, was also elevated in infected cells, suggesting that the perinuclear localization of the growing PV might be detected by the host cells as a defective vesicle fusion event. Alternatively, it may hijack the mitophagy membrane fusing machinery to establish a host mitochondrial-parasite membrane interface (Fig. 7). This speculation is supported by the finding of elevated TOMM20, which was shown to appear on surfaces of lysosomal-mitochondrial contact interfaces (Wong et al., 2018). These molecular insights provide a potential mechanistic basis for the frequently observed microsporidial protoplasmic extensions and multiple forms of tubular appendages that interface with host organelles (Cali et al., 1998; Takvorian and Cali, 1983).

Further experiments need to focus on how *E. intestinalis* avoids detection and degradation by host machinery while affecting the dynamics of cellular organelles through mitochondrial and lysosomal interactions. In addition, the parasitic proteins responsible for engaging the various cellular organelles need to be identified and

characterized. While our study provides a detailed ultrastructural study and molecular characterization of physiologically relevant microsporidian infection, further advances in sequencing techniques, such as sequencing at the single-cell level, could both refine the pathways specific to microsporidian infected cells and map out the development of pathogenesis.

#### **MATERIALS AND METHODS**

#### Cells and reagents for E. intestinalis culture

*E. intestinalis* was initially grown in rabbit kidney cells (RK-13; ATCC-CCL-37), that were cultured in minimum essential medium Eagle (MEM) containing 10% fetal bovine serum (FBS) penicillin-streptomycin (Thermo Fisher Scientific) at 37°C with 5%  $\rm CO_2$ . The medium from RK-13 cultures infected with *E. intestinalis* was removed weekly during medium changes and spores were collected from this medium, purified by passing them through 5  $\mu$ m size filter (Millex, Ireland) to remove host cells, concentrated by centrifugation (5000 g for 5 min), and stored in sterile distilled water at 4°C. Spores were also obtained from disrupted infected cells. The medium was removed and 1 ml of 0.25% (w/v) trypsin and 0.5% EDTA dissolved in phosphate-buffered saline (PBS) solution was added to the flask, covering the monolayer, for 5–10 min. Cells were released by streaming MEM from a pipette and discharging it onto the monolayer. The cells were collected and spores purified as described above.

Caco2 cells (ATCC-HTB-37) were grown in 25 cm² flasks in MEM containing 20% FBS, 1% penicillin-streptomycin (Thermo Fisher Scientific) at 37°C with 5% CO₂. Additionally, cells were also grown in two-well cover glass chamber wells. When confluent, several wells of cells were infected with 100 μl of ~106 spores/ml solution and maintained for 14 days. Uninfected and *E. intestinalis*-infected Caco2 cells were fixed with 4% paraformaldehyde and stained for F-actin with phalloidin–Alexa Fluor 488, and Calcofluor White 2MR (American Cyanamid Corp., Princeton, NJ) for detection of chitin with a Nikon T2000 fluorescence microscopy. Lysotracker (Green DND-26; Thermo Fisher Scientific, L7526) and Mitotracker (CM-H₂Xros; Thermo Fisher Scientific, M7513) were used according to manufacturer's recommendation to stain lysosomes and mitochondria, respectively. Fluorescent puncta events were counted per field for Mitotracker.

# Preparation for electron microscopy observation of Caco2 cells and RNA isolation

Four flasks of Caco2 cells were confluent after 7 days. Two flasks were maintained uninfected and two flasks were each infected with 200  $\mu l$  of  $10^6$  spores/ml solution and maintained for an additional 7 days. The cells of both uninfected and infected flasks were then split and added to four flasks. At 14 days post exposure, the infected cells and uninfected cells were both harvested and prepared for EM and RNA extraction, respectively.

#### **Transmission electron microscopy**

For TEM, individual samples of infected and uninfected cells were placed in microfuge tubes. The tubes were then centrifuged at 5000 *g* for 30 s to obtain a pellet of cells as previously described (Cali et al., 2002; Takvorian et al., 2020). The resulting pellets were fixed for 20 min in room temperature (RT) 2.5% glutaraldehyde in 0.1 M sodium cacodylate buffer. After 20 min, the RT fixative was removed and fresh 4°C fixative was added and stored overnight. The pellet was rinsed in 0.1 M sodium cacodylate buffer and post-fixed in 1% buffered OsO<sub>4</sub> overnight. The post-fixed pellets were dehydrated through a graded series of ethanol, transitioned into propylene oxide, and embedded in Epon LX-112 resin. Thin sections were stained with uranyl acetate and lead citrate. The samples were observed with an FEI Tecnai 12 TEM (FEI, Hillsboro, OR) and images recorded with a OneView 16 Megapixel digital camera (Gatan, Pleasanton, CA) at the Rutgers, Newark Electron Microscopy Facility.

#### RNA isolation and bulk RNA-seq analysis

The Caco2 cells of both uninfected and infected flasks were split and added to four flasks at 7 days post exposure. At 14 days post exposure, the infected cells and uninfected cells were both harvested and prepared for RNA extraction. RNA isolation was conducted using RNeasy Mini Kit (Qiagen,

Catalog No. 74104) according to the manufacturer's instructions. The quality of RNA was first checked using Agilent 2200 TapeStation System (Agilent Technologies, Santa Clara, CA). All the RNA samples had an RNA integrity number (RIN) of >9.0 and were used for subsequent processing. The maximum recommended concentration was used as an input and they were subjected to oligo(dT)-based mRNA isolation using an NEBNext poly(A) mRNA Magnetic Isolation Module (New England BioLabs, Ipswich, MA). Illumina compatible RNAseq libraries were then prepared using an NEBNext Ultra II RNA Library Prep Kit (New England BioLabs, Ipswich, MA). AMPureXP beads (Beckman Coulter, Brea, CA) were used to purify cDNA libraries. The quality and the size distribution of the libraries were determined by TapeStation and were quantified using Qubit Fluorometer (Invitrogen). Barcoded libraries were pooled at equimolar ratios and sequenced on Illumina NextSeq 500 platform (Illumina, San Diego, CA) with 1×75 configuration. Demultiplexing of raw data into Fastq files was undertaken using bcl2fastq (Illumina, San Diego, CA). Fastq files were analyzed using Partek® software. Copyright, Partek Inc. Partek and all other Partek Inc. product or service names are registered trademarks or trademarks of Partek Inc., St Louis, MO, USA. For gene set enrichment analysis (GSEA) (Subramanian et al., 2005), the molecular signature database (MSigDB) GO Biological Process (http://www.gsea-msigdb.org/ gsea/msigdb/collections.jsp) was used to generate enrichment plots and heatmaps to determine significance of differential expression between conditions. One thousand permutations were performed for each gene list tested; normalized enrichment scores (NES) and nominal P-values are reported for gene signatures. Heatmap Z-scores are centered and normalized around 1.5 standard deviations from the mean. Heatmaps generated by GSEA are on a relative min max scale. The nominal P-value of <0.05 was considered to indicate significant enrichment. The Wnt BetaCatenin and IL6 networks were generated through the use of IPA (QIAGEN Inc., https:// www.qiagenbioinformatics.com/products/ingenuity-pathway-analysis).

#### Acknowledgements

The authors thank Seema Husain (The Genomics Center) for helping with bulk RNA sequencing analysis.

### Competing interests

The authors declare no competing or financial interests.

#### Author contributions

Conceptualization: J.F., P.M.T., A.C., N.G.; Methodology: J.F., P.M.T.; Formal analysis: J.F., P.M.T.; Investigation: J.F.; Resources: L.M.W.; Writing - original draft: J.F., P.M.T., A.C., N.G.; Writing - review & editing: J.F., P.M.T., L.M.W., A.C., N.G.; Supervision: L.M.W., A.C., N.G.; Funding acquisition: L.M.W., N.G.

# Funding

This work was supported by the National Institutes of Health (NIH) (R01DK102934, R01DK119198, R01AT010243), National Science Foundation (NSF/BIO/IDBR; 1353890 and 1952823) to N.G., NIH R01AI124753 to L.M.W., and a New Jersey Commission on Cancer (NJCCR) fellowship (DCHS19PPC038 to J.F.). Deposited in PMC for release after 12 months.

### Data availability

The bulk RNA-seq data generated in this study were deposited in Gene Expression Omnibus (GEO) with accession number GSE167249.

#### Supplementary information

Supplementary information available online at https://jcs.biologists.org/lookup/doi/10.1242/jcs.253757.supplemental

#### Peer review history

The peer review history is available online at

https://jcs.biologists.org/lookup/doi/10.1242/jcs.253757.reviewer-comments.pdf

#### References

- Aguet, F., Antonescu, C. N., Mettlen, M., Schmid, S. L. and Danuser, G. (2013).
  Advances in analysis of low signal-to-noise images link dynamin and AP2 to the functions of an endocytic checkpoint. *Dev. Cell* 26, 279-291. doi:10.1016/j.devcel.
  2013.06.019
- Akiyama, J., Okamoto, R., Iwasaki, M., Zheng, X., Yui, S., Tsuchiya, K., Nakamura, T. and Watanabe, M. (2010). Delta-like 1 expression promotes goblet

- cell differentiation in Notch-inactivated human colonic epithelial cells. *Biochem. Biophys. Res. Commun.* **393**, 662-667. doi:10.1016/j.bbrc.2010.02.048
- An, J., Shi, J., He, Q., Lui, K., Liu, Y., Huang, Y. and Sheikh, M. S. (2012). CHCM1/ CHCHD6, novel mitochondrial protein linked to regulation of mitofilin and mitochondrial cristae morphology. *J. Biol. Chem.* 287, 7411-7426. doi:10.1074/ ibc.M111.277103
- Andreu-Ballester, J. C., Garcia-Ballesteros, C., Amigo, V., Ballester, F., Gil-Borrás, R., Catalán-Serra, I., Magnet, A., Fenoy, S., del Aguila, C., Ferrando-Marco, J. et al. (2013). Microsporidia and its relation to Crohn's disease. A retrospective study. PLoS ONE 8, e62107. doi:10.1371/journal.pone.0062107
- Arvidsson, Y., Andersson, E., Bergström, A., Andersson, M. K., Altiparmak, G., Illerskog, A.-C., Ahlman, H., Lamazhapova, D. and Nilsson, O. (2008). Amyloid precursor-like protein 1 is differentially upregulated in neuroendocrine tumours of the gastrointestinal tract. *Endocr. Relat. Cancer* 15, 569-581. doi:10. 1677/ERC-07-0145
- Band, A. M. and Kuismanen, E. (2005). Localization of plasma membrane t-SNAREs syntaxin 2 and 3 in intracellular compartments. BMC Cell Biol. 6, 26. doi:10.1186/1471-2121-6-26
- Barrière, G., Rabinovitch-Chable, H., Cook-Moreau, J., Faucher, K., Rigaud, M. and Sturtz, F. (2004). PHGPx overexpression induces an increase in COX-2 activity in colon carcinoma cells. *Anticancer Res.* **24**, 1387-1392.
- Bauer, M. F., Gempel, K., Reichert, A. S., Rappold, G. A., Lichtner, P., Gerbitz, K.-D., Neupert, W., Brunner, M. and Hofmann, S. (1999). Genetic and structural characterization of the human mitochondrial inner membrane translocase. *J. Mol. Biol.* 289, 69-82. doi:10.1006/jmbi.1999.2751
- Becnel, J. J., Takvorian, P. M. and Cali, A. (2014). Checklist of available generic names for microsporidia with type species and type hosts. In *Microsporidia Pathogens of Opportunity* (eds Weiss L. M., Becnel J. J.), pp. 671-686. Hoboken, NJ, Wiley Blackwell Press. doi:10.1002/9781118395264. Appendix A.
- Bednarska, M., Bajer, A., Siński, E., Wolska-Kuśnierz, B., Samoliński, B. and Graczyk, T. K. (2014). Occurrence of intestinal microsporidia in immunodeficient patients in Poland. *Ann. Agric. Environ. Med.* 21, 244-248. doi:10.5604/1232-1966.1108584
- Bömer, U., Rassow, J., Zufall, N., Pfanner, N., Meijer, M. and Maarse, A. C. (1996). The preprotein translocase of the inner mitochondrial membrane: evolutionary conservation of targeting and assembly of Tim17. *J. Mol. Biol.* 262, 389-395. doi:10.1006/jmbi.1996.0522
- Botts, M. R., Cohen, L. B., Probert, C. S., Wu, F. and Troemel, E. R. (2016).
  Microsporidia intracellular development relies on Myc interaction network transcription factors in the host. G3 6, 2707-2716. doi:10.1534/g3.116.029983
- Bourgonje, A. R., Abdulle, A. E., Timens, W., Hillebrands, J. L., Navis, G. J., Gordijn, S. J., Bolling, M. C., Dijkstra, G., Voors, A. A., Osterhaus, A. D. et al. (2020). Angiotensin-converting enzyme 2 (ACE2), SARS-CoV-2 and the pathophysiology of coronavirus disease 2019 (COVID-19). *J. Pathol.* **251**, 228-248. doi:10.1002/path.5471
- Burré, J., Sharma, M., Tsetsenis, T., Buchman, V., Etherton, M. R. and Südhof, T. C. (2010). Alpha-synuclein promotes SNARE-complex assembly in vivo and in vitro. *Science* 329, 1663-1667. doi:10.1126/science.1195227
- Cali, A. and Takvorian, P. (2004). The microsporidia: pathology in man and occurrence in nature. S. E. Asian J. Trop. Med. Public Health 35, 58-64.
- Cali, A. and Takvorian, P. M. (2014). Developmental morphology and life cycles of the microsporidia. In *Microsporidia - Pathogens of Opportunity* (eds Weiss L. M., Becnel J. J.), pp. 71-133. Hoboken, NJ, Wiley Blackwell Press. doi:10.1002/ 9781118395264.ch2
- Cali, A., Kotler, D. P. and Orenstein, J. M. (1993). Septata intestinalis N. G., N. Sp., an intestinal microsporidian associated with chronic diarrhea and dissemination in AIDS patients. *J. Eukaryot. Microbiol.* **40**, 101-112. doi:10.1111/j.1550-7408. 1993 tb04889 x
- Cali, A., Takvorian, P. M., Lewin, S., Rendel, M., Sian, C. S., Wittner, M., Tanowitz, H. B., Keohane, E. and Weiss, L. M. (1998). Brachiola vesicularum, n. g., n. sp., a new microsporidium associated with AIDS and myositis. *J. Eukaryot. Microbiol.* 45, 240-251. doi:10.1111/j.1550-7408.1998.tb04532.x
- Cali, A., Weiss, L. M. and Takvorian, P. M. (2002). Brachiola algerae spore membrane systems, their activity during extrusion, and a new structural entity, the multilayered interlaced network, associated with the polar tube and the sporoplasm. J. Eukaryot. Microbiol. 49, 164-174. doi:10.1111/j.1550-7408.2002. tb00361.x
- Candy, P. A., Phillips, M. R., Redfern, A. D., Colley, S. M., Davidson, J. A., Stuart, L. M., Wood, B. A., Zeps, N. and Leedman, P. J. (2013). Notch-induced transcription factors are predictive of survival and 5-fluorouracil response in colorectal cancer patients. *Br. J. Cancer* 109, 1023-1030. doi:10.1038/bjc.2013. 431
- Cha, M.-K. and Kim, I.-H. (2009). Preferential overexpression of glutaredoxin3 in human colon and lung carcinoma. *Cancer Epidemiol.* 33, 281-287. doi:10.1016/j. canep.2009.08.006
- Cho, H. and Kehrl, J. H. (2007). Localization of Giα proteins in the centrosomes and at the midbody: implication for their role in cell division. *J. Cell Biol.* 178, 245-255. doi:10.1083/jcb.200604114
- Cragg, M. S., Chan, H. T. C., Fox, M. D., Tutt, A., Smith, A., Oscier, D. G., Hamblin, T. J. and Glennie, M. J. (2002). The alternative transcript of CD79b is

- overexpressed in B-CLL and inhibits signaling for apoptosis. *Blood* **100**, 3068-3076. doi:10.1182/blood.V100.9.3068
- Crawley, S. W., Shifrin, D. A., Jr., Grega-Larson, N. E., McConnell, R. E., Benesh, A. E., Mao, S., Zheng, Y., Zheng, Q. Y., Nam, K. T., Millis, B. A. et al. (2014). Intestinal brush border assembly driven by protocadherin-based intermicrovillar adhesion. *Cell* 157, 433-446. doi:10.1016/j.cell.2014.01.067
- Darshi, M., Mendiola, V. L., Mackey, M. R., Murphy, A. N., Koller, A., Perkins, G. A., Ellisman, M. H. and Taylor, S. S. (2011). ChChd3, an inner mitochondrial membrane protein, is essential for maintaining crista integrity and mitochondrial function. J. Biol. Chem. 286, 2918-2932. doi:10.1074/jbc.M110.171975
- Desportes, I., Le Charpentier, Y., Galian, A., Bernard, F., Cochand-Priollet, B., Lavergne, A., Ravisse, P. and Modigliani, R. (1985). Occurrence of a new microsporidan: *Enterocytozoon bieneusi* n.g., n. sp., in the enterocytes of a human patient with AIDS. *J. Protozool.* 32, 250-254. doi:10.1111/j.1550-7408. 1985.tb03046.x
- Didier, E. S. and Weiss, L. M. (2006). Microsporidiosis: current status. *Curr. Opin. Infect. Dis.* **19**, 485-492. doi:10.1097/01.gco.0000244055.46382.23
- Drover, V. A., Ajmal, M., Nassir, F., Davidson, N. O., Nauli, A. M., Sahoo, D., Tso, P. and Abumrad, N. A. (2005). CD36 deficiency impairs intestinal lipid secretion and clearance of chylomicrons from the blood. *J. Clin. Invest.* 115, 1290-1297. doi:10.1172/JCl21514
- El Fakhry, Y., Achbarou, A., Franetich, J.-F., Desportes-Livage, I. and Mazier, D. (2001). Dissemination of Encephalitozoon intestinalis, a causative agent of human microsporidiosis, in IFN-gamma receptor knockout mice. *Parasite Immunol.* 23, 19-25. doi:10.1046/j.1365-3024.2001.00351.x
- Fayer, R. and Santin-Duran, M. (2014). Epidemiology of microsporidia in human infections. In *Microsporidia - Pathogens of Opportunity* (eds Weiss L. M., Becnel J. J.), pp. 135-164. Hoboken, NJ, Wiley Blackwell Press. doi:10.1002/ 9781118395264.ch3
- **Ferguson, S. and Lucocq, J.** (2019). The invasive cell coat at the microsporidian Trachipleistophora hominis—host cell interface contains secreted hexokinases. *MicrobiologyOpen* **8**, e00696. doi:10.1002/mbo3.696
- **Foucault, C. and Drancourt, M.** (2000). Actin mediates Encephalitozoon intestinalis entry into the human enterocyte-like cell line, Caco2. *Microb. Pathog.* **28**, 51-58. doi:10.1006/mpat.1999.0329
- Fraering, P. C., Ye, W., Strub, J.-M., Dolios, G., LaVoie, M. J., Ostaszewski, B. L., van Dorsselaer, A., Wang, R., Selkoe, D. J. and Wolfe, M. S. (2004). Purification and characterization of the human γ-secretase complex. *Biochemistry* 43, 9774-9789. doi:10.1021/bi0494976
- Gao, N. and Kaestner, K. H. (2010). Cdx2 regulates endo-lysosomal function and epithelial cell polarity. *Genes Dev.* **24**, 1295-1305. doi:10.1101/gad.1921510
- Gao, L., Cueto, M. A., Asselbergs, F. and Atadja, P. (2002). Cloning and functional characterization of HDAC11, a novel member of the human histone deacetylase family. J. Biol. Chem. 277, 25748-25755. doi:10.1074/jbc.M111871200
- Genin, E. C., Plutino, M., Bannwarth, S., Villa, E., Cisneros-Barroso, E., Roy, M., Ortega-Vila, B., Fragaki, K., Lespinasse, F., Pinero-Martos, E. et al. (2016). CHCHD10 mutations promote loss of mitochondrial cristae junctions with impaired mitochondrial genome maintenance and inhibition of apoptosis. EMBO Mol. Med. 8, 58-72. doi:10.15252/emmm.201505496
- Goldberg, M., Peshkovsky, C., Shifteh, A. and Al-Awqati, Q. (2000). μ-Protocadherin, a novel developmentally regulated protocadherin with mucin-like domains. *J. Biol. Chem.* **275**, 24622-24629. doi:10.1074/jbc.M000234200
- Grossmann, D., Berenguer-Escuder, C., Chemla, A., Arena, G. and Kruger, R. (2020). The emerging role of RHOT1/Miro1 in the pathogenesis of Parkinson's disease. Front. Neurol. 11, 587. doi:10.3389/fneur.2020.00587
- Gremel, G., Djureinovic, D., Niinivirta, M., Laird, A., Ljungqvist, O., Johannesson, H., Bergman, J., Edqvist, P.-H., Navani, S., Khan, N. et al. (2017). A systematic search strategy identifies cubilin as independent prognostic marker for renal cell carcinoma. *BMC Cancer* 17, 9. doi:10.1186/s12885-016-3030-6
- Guilmeau, S., Flandez, M., Mariadason, J. M. and Augenlicht, L. H. (2010). Heterogeneity of Jagged1 expression in human and mouse intestinal tumors: implications for targeting Notch signaling. *Oncogene* 29, 992-1002. doi:10.1038/onc.2009.393
- Hacker, C., Howell, M., Bhella, D. and Lucocq, J. (2014). Strategies for maximizing ATP supply in the microsporidian Encephalitozoon cuniculi: direct binding of mitochondria to the parasitophorous vacuole and clustering of the mitochondrial porin VDAC. Cell. Microbiol. 16, 565-579. doi:10.1111/cmi.12240
- Hamamci, B., Çetinkaya, U., Berk, V., Kaynar, L., Kuk, S. and Yazar, S. (2015).
  Prevalence of Encephalitozoon intestinalis and Enterocytozoon bieneusi in cancer patients under chemotherapy. *Mikrobiyol. Bul.* 49, 105-113. doi:10.5578/mb.8787
- Han, B., Ma, Y., Tu, V., Tomita, T., Mayoral, J., Williams, T., Horta, A., Huang, H. and Weiss, L. M. (2019). Microsporidia interact with host cell mitochondria via voltage-dependent anion channels using sporoplasm surface protein 1. *mBio* 10, e01944-19. doi:10.1128/mBio.01944-19.
- Han, B., Takvorian, P. M. and Weiss, L. M. (2020). Invasion of host cells by microsporidia. *Front. Microbiol.* 11, 172. doi:10.3389/fmicb.2020.00172

- Han, B. and Weiss, L. M. (2017). Microsporidia: Obligate Intracellular Pathogens Within the Fungal Kingdom. *Microbiol Spectr* 5. doi:10.1128/microbiolspec. FUNK-0018-2016.
- Hartskeerl, R. A., Van Gool, T., Schuitema, A. R. J., Didier, E. S. and Terpstra, W. J. (1995). Genetic and immunological characterization of the microsporidian Septata intestinalis Cali, Kotler and Orenstein, 1993: reclassification to Encephalitozoon intestinalis. *Parasitology* 110 , 277-285. doi:10.1017/S0031182000080860
- Hayashi, H. and Yamashita, Y. (2012). Role of N-glycosylation in cell surface expression and protection against proteolysis of the intestinal anion exchanger SLC26A3. Am. J. Physiol. Cell Physiol. 302, C781-C795. doi:10.1152/ajpcell. 00165.2011
- Horn, H. F., Brownstein, Z., Lenz, D. R., Shivatzki, S., Dror, A. A., Dagan-Rosenfeld, O., Friedman, L. M., Roux, K. J., Kozlov, S., Jeang, K.-T. et al. (2013). The LINC complex is essential for hearing. *J. Clin. Invest.* **123**, 740-750. doi:10.1172/JCl66911
- Hsu, N., Young, L. S. and Bermudez, L. E. (1995). Response to stimulation with recombinant cytokines and synthesis of cytokines by murine intestinal macrophages infected with the Mycobacterium avium complex. *Infect. Immun.* 63, 528-533. doi:10.1128/IAI.63.2.528-533.1995
- Hsu, N.-Y., Ilnytska, O., Belov, G., Santiana, M., Chen, Y.-H., Takvorian, P. M., Pau, C., van der Schaar, H., Kaushik-Basu, N., Balla, T. et al. (2010). Viral reorganization of the secretory pathway generates distinct organelles for RNA replication. Cell 141. 799-811. doi:10.1016/j.cell.2010.03.050
- Hurst, S., Baggett, A., Csordas, G. and Sheu, S. S. (2019). SPG7 targets the m-AAA protease complex to process MCU for uniporter assembly, Ca<sup>2+</sup> influx, and regulation of mitochondrial permeability transition pore opening. *J. Biol. Chem.* 294, 10807-10818. doi:10.1074/jbc.RA118.006443
- Ikari, A., Tonegawa, C., Sanada, A., Kimura, T., Sakai, H., Hayashi, H., Hasegawa, H., Yamaguchi, M., Yamazaki, Y., Endo, S. et al. (2014). Tight junctional localization of claudin-16 is regulated by syntaxin 8 in renal tubular epithelial cells. J. Biol. Chem. 289, 13112-13123. doi:10.1074/jbc.M113.541193
- Junn, E., Jang, W. H., Zhao, X., Jeong, B. S. and Mouradian, M. M. (2009). Mitochondrial localization of DJ-1 leads to enhanced neuroprotection. *J. Neurosci. Res.* 87, 123-129. doi:10.1002/jnr.21831
- Kadlecova, Z., Spielman, S. J., Loerke, D., Mohanakrishnan, A., Reed, D. K. and Schmid, S. L. (2017). Regulation of clathrin-mediated endocytosis by hierarchical allosteric activation of AP2. J. Cell Biol. 216, 167-179. doi:10.1083/jcb.201608071
- Keeling, P. J., Fast, N. M. and Corradi, N. (2014). Microsporidian genome structure and function. In *Microsporidia - Pathogens of Opportunity* (eds Weiss L. M., Becnel J. J.), pp. 71-133. Hoboken, NJ, Wiley Blackwell Press. doi:10.1002/ 9781118395264.ch7
- Knowles, B. C., Weis, V. G., Yu, S., Roland, J. T., Williams, J. A., Alvarado, G. S., Lapierre, L. A., Shub, M. D., Gao, N. and Goldenring, J. R. (2015). Rab11a regulates Syntaxin 3 localization and microvillus assembly in enterocytes. *J. Cell Sci.* 128, 1617-1626. doi:10.1242/ics.163303
- Koh, E., Kim, Y. K., Shin, D. and Kim, K. S. (2018). MPC1 is essential for PGC-1alpha-induced mitochondrial respiration and biogenesis. *Biochem. J.* 475, 1687-1699. doi:10.1042/BCJ20170967.
- Krishnamurthy, P. C., Du, G., Fukuda, Y., Sun, D., Sampath, J., Mercer, K. E., Wang, J., Sosa-Pineda, B., Murti, K. G. and Schuetz, J. D. (2006). Identification of a mammalian mitochondrial porphyrin transporter. *Nature* **443**, 586-589. doi:10. 1038/nature05125
- Kuo, C.-J., Hansen, M. and Troemel, E. (2018). Autophagy and innate immunity: insights from invertebrate model organisms. Autophagy 14, 233-242. doi:10.1080/ 15548627.2017.1389824
- Lee, W. S., Wells, R. G., Sabbag, R. V., Mohandas, T. K. and Hediger, M. A. (1993). Cloning and chromosomal localization of a human kidney cDNA involved in cystine, dibasic, and neutral amino acid transport. *J. Clin. Invest.* 91, 1959-1963. doi:10.1172/JCI116415
- Leitch, G. J., Ward, T. L., Shaw, A. P. and Newman, G. (2005). Apical spore phagocytosis is not a significant route of infection of differentiated enterocytes by Encephalitozoon intestinalis. *Infect. Immun.* 73, 7697-7704. doi:10.1128/IAI.73. 11.7697-7704.2005
- Li, Y., Lim, S., Hoffman, D., Aspenstrom, P., Federoff, H. J. and Rempe, D. A. (2009). HUMMR, a hypoxia- and HIF-1alpha-inducible protein, alters mitochondrial distribution and transport. *J. Cell Biol.* 185, 1065-1081. doi:10. 1083/icb.200811033
- Lv, L., Liu, H.-G., Dong, S.-Y., Yang, F., Wang, Q.-X., Guo, G.-L., Pan, Y.-F. and Zhang, X.-H. (2016). Upregulation of CD44v6 contributes to acquired chemoresistance via the modulation of autophagy in colon cancer SW480 cells. *Tumour Biol.* **37**, 8811-8824. doi:10.1007/s13277-015-4755-6
- Mahon, M. J., Donowitz, M., Yun, C. C. and Segre, G. V. (2002). Na<sup>+</sup>/H<sup>+</sup> exchanger regulatory factor 2 directs parathyroid hormone 1 receptor signalling. *Nature* 417, 858-861. doi:10.1038/nature00816
- Moise, A. R., Kuksa, V., Imanishi, Y. and Palczewski, K. (2004). Identification of all-trans-retinol:all-trans-13,14-dihydroretinol saturase. J. Biol. Chem. 279, 50230-50242. doi:10.1074/jbc.M409130200
- Morgan, J. T., Pfeiffer, E. R., Thirkill, T. L., Kumar, P., Peng, G., Fridolfsson, H. N., Douglas, G. C., Starr, D. A. and Barakat, A. I. (2011). Nesprin-3 regulates

- endothelial cell morphology, perinuclear cytoskeletal architecture, and flow-induced polarization. *Mol. Biol. Cell* **22**, 4324-4334. doi:10.1091/mbc.e11-04-0287
- Morimoto, A., Shibuya, H., Zhu, X., Kim, J., Ishiguro, K.-I., Han, M. and Watanabe, Y. (2012). A conserved KASH domain protein associates with telomeres, SUN1, and dynactin during mammalian meiosis. *J. Cell Biol.* 198, 165-172. doi:10.1083/jcb.201204085
- Moro, F., Sirrenberg, C., Schneider, H.-C., Neupert, W. and Brunner, M. (1999). The TIM17-23 preprotein translocase of mitochondria: composition and function in protein transport into the matrix. *EMBO J.* 18, 3667-3675. doi:10.1093/emboj/18. 13 3667
- Moss, A. C., Lawlor, G., Murray, D., Tighe, D., Madden, S. F., Mulligan, A.-M., Keane, C. O., Brady, H. R., Doran, P. P. and MacMathuna, P. (2006). ETV4 and Myeov knockdown impairs colon cancer cell line proliferation and invasion. *Biochem. Biophys. Res. Commun.* **345**, 216-221. doi:10.1016/j.bbrc.2006.04.094
- Nigrelli, R. F. (1946). Studies on the marine resources of southern New England. V. Parasites and diseases of the ocean pout, Macrozoarcts americanus. *Bull. Bingham Oceanographic Collection* **9**, 187-221.
- Orenstein, J. M., Chiang, J., Steinberg, W., Smith, P. D., Rotterdam, H. and Kotler, D. P. (1990). Intestinal microsporidiosis as a cause of diarrhea in human immunodeficiency virus-infected patients: a report of 20 cases. *Hum. Pathol.* 21, 475-481. doi:10.1016/0046-8177(90)90003-N
- Peng, X., Pan, K., Zhao, W., Zhang, J., Yuan, S., Wen, X., Zhou, W. and Yu, Z. (2018). NPTX1 inhibits colon cancer cell proliferation through down-regulating cyclin A2 and CDK2 expression. *Cell Biol. Int.* 42, 589-597. doi:10.1002/cbin. 10935
- Peters, U., Chatterjee, N., Hayes, R. B., Schoen, R. E., Wang, Y., Chanock, S. J. and Foster, C. B. (2008). Variation in the selenoenzyme genes and risk of advanced distal colorectal adenoma. *Cancer Epidemiol. Biomark. Prev.* 17, 1144-1154. doi:10.1158/1055-9965.EPI-07-2947
- Pinho, M. P., Migliori, I. K., Flatow, E. A. and Barbuto, J. A. M. (2014). Dendritic cell membrane CD83 enhances immune responses by boosting intracellular calcium release in T lymphocytes. *J. Leukoc. Biol.* 95, 755-762. doi:10.1189/jlb. 0413239
- Qiu, A., Jansen, M., Sakaris, A., Min, S. H., Chattopadhyay, S., Tsai, E., Sandoval, C., Zhao, R., Akabas, M. H. and Goldman, I. D. (2006). Identification of an intestinal folate transporter and the molecular basis for hereditary folate malabsorption. *Cell* 127, 917-928. doi:10.1016/j.cell.2006.09.041
- Raynaud, L., Delbac, F., Broussolle, V., Rabodonirina, M., Girault, V., Wallon, M., Cozon, G., Vivares, C. P. and Peyron, F. (1998). Identification of Encephalitozoon intestinalis in travelers with chronic diarrhea by specific PCR amplification. *J. Clin. Microbiol.* 36, 37-40. doi:10.1128/JCM.36.1.37-40.1998
- Reddy, K. C., Dror, T., Underwood, R. S., Osman, G. A., Elder, C. R., Desjardins, C. A., Cuomo, C. A., Barkoulas, M. and Troemel, E. R. (2019). Antagonistic paralogs control a switch between growth and pathogen resistance in *C. elegans*. *PLoS Pathog.* 15, e1007528. doi:10.1371/journal.ppat.1007528
- Santiana, M., Takvorian, P. M., Altan-Bonnet, N. and Cali, A. (2016). A novel fluorescent labeling method enables monitoring of spatio-temporal dynamics of developing microsporidia. *J. Eukaryot. Microbiol.* 63, 318-325. doi:10.1111/jeu. 12281
- Sazanov, L. A. (2015). A giant molecular proton pump: structure and mechanism of respiratory complex I. Nat. Rev. Mol. Cell Biol. 16, 375-388. doi:10.1038/nrm3997
- Scanlon, M., Leitch, G. J., Visvesvara, G. S. and Shaw, A. P. (2004). Relationship between the host cell mitochondria and the parasitophorous vacuole in cells infected with Encephalitozoon microsporidia. *J. Eukaryot. Microbiol.* **51**, 81-87. doi:10.1111/j.1550-7408.2004.tb00166.x
- Schlingmann, K. P., Weber, S., Peters, M., Niemann Nejsum, L., Vitzthum, H., Klingel, K., Kratz, M., Haddad, E., Ristoff, E., Dinour, D. et al. (2002). Hypomagnesemia with secondary hypocalcemia is caused by mutations in TRPM6, a new member of the TRPM gene family. *Nat. Genet.* **31**, 166-170. doi:10.1038/ng889
- Stewart-Hutchinson, P. J., Hale, C. M., Wirtz, D. and Hodzic, D. (2008). Structural requirements for the assembly of LINC complexes and their function in cellular mechanical stiffness. *Exp. Cell Res.* **314**, 1892-1905. doi:10.1016/j.yexcr.2008. 02.022
- Subramanian, A., Tamayo, P., Mootha, V. K., Mukherjee, S., Ebert, B. L., Gillette, M. A., Paulovich, A., Pomeroy, S. L., Golub, T. R., Lander, E. S. et al. (2005). Gene set enrichment analysis: a knowledge-based approach for interpreting

- genome-wide expression profiles. *Proc. Natl. Acad. Sci. USA* **102**, 15545-15550. doi:10.1073/pnas.0506580102.
- **Takvorian, P. M. and Cali, A.** (1983). Appendages associated with Glugea stephani, a microsporidan found in flounder. *J. Protozool.* **30**, 251-256. doi:10. 1111/j.1550-7408.1983.tb02911.x
- Takvorian, P. M., Han, B., Cali, A., Rice, W. J., Gunther, L., Macaluso, F. and Weiss, L. M. (2020). An ultrastructural study of the extruded polar tube of *Anncaliia algerae* (Microsporidia). *J. Eukaryot. Microbiol.* 67, 28-44. doi:10.1111/jeu.12751
- Troemel, E. R. (2011). New models of microsporidiosis: infections in Zebrafish, C. elegans, and honey bee. PLoS Pathog. 7, e1001243. doi:10.1371/journal.ppat. 1001243
- Valdez, A. C., Cabaniols, J. P., Brown, M. J. and Roche, P. A. (1999). Syntaxin 11 is associated with SNAP-23 on late endosomes and the trans-Golgi network. *J. Cell Sci.* **112**, 845-854.
- van Gool, T., Vetter, J. C. M., Weinmayr, B., Van Dam, A., Derouin, F. and Dankert, J. (1997). High seroprevalence of Encephalitozoon species in immunocompetent subjects. J. Infect. Dis. 175, 1020-1024. doi:10.1086/513963
- Visvesvara, G. S. (2002). In vitro cultivation of microsporidia of clinical importance. Clin. Microbiol. Rev. 15, 401-413. doi:10.1128/CMR.15.3.401-413.2002
- Watson, A. K., Williams, T. A., Williams, B. A. P., Moore, K. A., Hirt, R. P. and Embley, T. M. (2015). Transcriptomic profiling of host-parasite interactions in the microsporidian Trachipleistophora hominis. *BMC Genomics* 16, 983. doi:10.1186/ s12864-015-1989-z
- Welsch, D. J., Creely, D. P., Hauser, S. D., Mathis, K. J., Krivi, G. G. and Isakson, P. C. (1994). Molecular cloning and expression of human leukotriene-C4 synthase. *Proc. Natl. Acad. Sci. USA* **91**, 9745-9749. doi:10.1073/pnas.91.21.9745
- Weiss, L. M. and Kim, K. (2020). Toxoplasma gondii: The Model Apicomplexan Perspectives and Methods Third Edition, Ch14, pp.1222, Academic Press, Elsevier Ltd. doi:10.1016/C2017-0-01845-1
- Williams, B. A. P., Dolgikh, V. V. and Sokolova, Y. Y. (2014). Microsporidian biochemistry and physiology. In *Microsporidia - Pathogens of Opportunity* (eds Weiss L. M., Becnel J. J.), pp. 245-260. Hoboken, NJ, Wiley Blackwell Press. doi:10.1002/9781118395264.ch9
- Willis, W. T., Miranda-Grandjean, D., Hudgens, J., Willis, E. A., Finlayson, J., De Filippis, E. A., Zapata Bustos, R., Langlais, P. R., Mielke, C. and Mandarino, L. J. (2018). Dominant and sensitive control of oxidative flux by the ATP-ADP carrier in human skeletal muscle mitochondria: effect of lysine acetylation. *Arch. Biochem. Biophys.* 647, 93-103. doi:10.1016/j.abb.2018.04.006
- Wong, Y. C., Ysselstein, D. and Krainc, D. (2018). Mitochondria-lysosome contacts regulate mitochondrial fission via RAB7 GTP hydrolysis. *Nature* 554, 382-386. doi:10.1038/nature25486
- Xian, H., Yang, Q., Xiao, L., Shen, H.-M. and Liou, Y.-C. (2019). STX17 dynamically regulated by Fis1 induces mitophagy via hierarchical macroautophagic mechanism. *Nat. Commun.* 10, 2059. doi:10.1038/s41467-019-10096-1
- Xu, J., Fang, J., Cheng, Z., Fan, L., Hu, W., Zhou, F. and Shen, H. (2018). Overexpression of the Kininogen-1 inhibits proliferation and induces apoptosis of glioma cells. J. Exp. Clin. Cancer Res. 37, 180. doi:10.1186/s13046-018-0833-0
- Yamamoto, H., Esaki, M., Kanamori, T., Tamura, Y., Nishikawa, S.-l. and Endo, T. (2002). Tim50 is a subunit of the TIM23 complex that links protein translocation across the outer and inner mitochondrial membranes. *Cell* 111, 519-528. doi:10. 1016/S0092-8674(02)01053-X
- Young, K. G., Pool, M. and Kothary, R. (2003). Bpag1 localization to actin filaments and to the nucleus is regulated by its N-terminus. *J. Cell Sci.* 116, 4543-4555. doi:10.1242/jcs.00764
- Zhang, Q., Ragnauth, C. D., Skepper, J. N., Worth, N. F., Warren, D. T., Roberts, R. G., Weissberg, P. L., Ellis, J. A. and Shanahan, C. M. (2005). Nesprin-2 is a multi-isomeric protein that binds lamin and emerin at the nuclear envelope and forms a subcellular network in skeletal muscle. *J. Cell Sci.* 118, 673-687. doi:10.1242/ics.01642
- Zhang, X., Lei, K., Yuan, X., Wu, X., Zhuang, Y., Xu, T., Xu, R. and Han, M. (2009). SUN1/2 and Syne/Nesprin-1/2 complexes connect centrosome to the nucleus during neurogenesis and neuronal migration in mice. *Neuron* **64**, 173-187. doi:10. 1016/j.neuron.2009.08.018
- Zhou, Q., Hao, L., Huang, W. and Cai, Z. (2016). The golgi-associated plant pathogenesis-related protein GAPR-1 enhances Type I interferon signaling pathway in response to toll-like receptor 4. *Inflammation* 39, 706-717. doi:10.1007/s10753-015-0297-8